ACS OMEGA

Open Access

http://pubs.acs.org/journal/acsodf

Article

Simulation Study of Coal Seam Gas Extraction Characteristics Based on Coal Permeability Evolution Model under Thermal Effect

Naifu Cao,* Pengfei Jing, Zhonggang Huo, Yuntao Liang, and Lang Zhang

Cite This: *ACS Omega* 2024, 9, 22871−22891

Read Online

ACCESS | Metrics & More | Article Recommendations

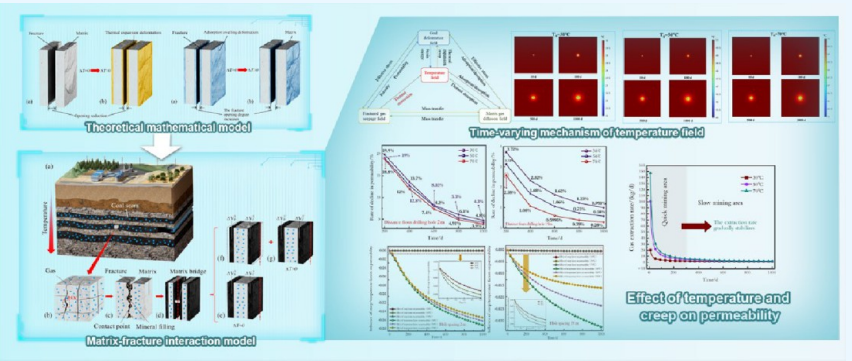

ABSTRACT: The permeability evolution law of high temperature and high stress coal seam is determined by the influence of multiphase coexistence and multifield coupling. In an environment greatly affected by disturbance and high temperature, the coal permeability model under the coupling of thermal and mechanical creep is not only a vital framework from which to examine gas migration law in multiphase and multifield coal seams but also an important theoretical foundation for gas control in coal seams. The influence of high-temperature environment on creep deformation and permeability is analyzed by several creep seepage tests under different temperature conditions.A mathematical model for the evolution of coal permeability considering the influence of temperature is established through the theory of matrix−crack interaction based on gas adsorption and desorption and thermal expansion deformation. Based on the permeability model under the coupling of thermal and mechanical creep, the numerical model of gas migration, seepage field, diffusion field, stress field, and temperature field is constructed, and the law of gas migration in coal seam under multifield coupling is explored. The influence law of thermal effect on gas extraction characteristics is analyzed, in which the time-varying mechanism of temperature field, the relationship between creep deformation and temperature and pressure, the influence of creep deformation on permeability, the dynamic distribution of gas pressure, and the change of gas extraction quantity are described in detail. It is concluded that the influence of temperature on permeability is much greater than that of creep deformation and that a high initial coal seam temperature is beneficial to gas extraction. It provides theoretical basis and technical guidance for the study of multifield coupled gas migration and coal seam gas treatment.

1. INTRODUCTION

At present, more than half of deep coal mines in China are high-gas mines.[1] In a deep high-gas mine, the gas concentration and pressure are greater in the coal seam, and the problem of gas outburst is becoming increasingly obvious.[2] The gas extraction of low-permeability coal seam in high-gas mine is faced with such problems as difficult extraction, small range, and high decay rate.[3] In deep high-gas mines located in China, over 90% of coal and gas outbursts transpire within low-permeability coal strata, characterized by permeabilities that vary between 10^{-6} and 10^{-7} μm^2.[4] At the same time, the coal seam gas permeability diminishes with increasing mining depth. Coal body deformation caused by high ground stress and high-temperature-induced deformation to enable thermal expansion also affect the desorption and adsorption of gas, having a substantial effect on the movement of gases within coal seams.[4,5] Temperature not only affects the reaction kinetics of gas desorption and adsorption processes but also affects the law of gas seepage in coal seams.[6,7]

With the deepening of deep mining work, the mining conditions of coal seams are increasingly complex and changeable, and the "three high" coal seams with high

Received: February 22, 2024
Revised: April 17, 2024
Accepted: April 22, 2024
Published: May 15, 2024

temperature, high gas, and high stress are gradually increasing.[8] The high temperature affects the gas and stress distribution in coal seam through exerting an influence on gas adsorption and desorption reactions in addition to coal body deformation, thus producing the intricate process of thermal and mechanical coupling between coal and rock.[8,9] Therefore, the change of the mechanical properties of coal under heat loss and stress has a great impact on practical engineering. At present, relevant research is mainly carried out in three aspects: mechanical properties of coal under thermal and mechanical coupling, creep, and thermal damage.

(1) *Thermal Coupling Mechanical Properties of Coal and Rock Mass.* From the perspective of basic theoretical experiments, it can be seen that coal body changes its physical and mechanical properties under the action of high temperature.[10] Heuze,[11] Glover et al.,[12] and Chopra[13] took coal rock as samples and found that the increase of temperature reduces its density. Zhang et al.[14] confirmed through high-temperature mechanical experiments on coal and rock that temperature increase exhibits a direct correlation with the porosity and permeability of coal and rock.

(2) *Study on Thermal and Mechanical Coupling Coal Creep.* In the study of thermal and mechanical coupling coal creep, the creep test at different temperatures is relatively concentrated. The constitutive relation of coal creep due to temperature's effect was obtained using a rock creep testing machine and high-temperature seepage system, and then this governing equation was used to characterize the creep of coal under different temperatures and stresses.[15]

(3) *Numerical Simulation of Coal Body Damage under Thermal−Mechanical Coupling.* Related study on damage to the coal body considering coupling under mechanical and thermal factors is more focused on the visualization of coal body cracks under the influence of high temperature through numerical simulation. Li et al.[16] used the elastic damage mechanism and thermoelastic theory combined with the isomerization characteristics of coal and rock at the mesoscopic level to obtain the thermodynamic coupling effect under the condition of damage to rock and coal due to thermal stress and built a mesoscopic thermodynamic coupling damage model. The stress distribution and failure characteristics of isotropic and anisotropic coal rock mass under thermal load were established by numerical simulation using the RFPA2D program.[17,18]

The findings of this study are crucial in establishing the mechanical properties and fracture laws of coal under heat loss.[19,20] The introduction of uniaxial and triaxial compression tests under the influence of temperature, the microscopic observation of heat-lost coal by scanning electron microscopy and nuclear magnetic technology,[21,22] and the exploration of the internal correlation between temperature and pore distribution and permeability through laboratory tests and numerical simulation provide an important theoretical framework that underpins the investigation of permeability evolution and porosity distribution under the coupling effect of thermal−mechanical creep.[23]

However, when examining the coal permeability evolution law based on thermal−mechanical coupling creep, most domestic and foreign scholars construct permeability models at normal temperature through seepage tests and numerical simulation methods or focus on the qualitative or quantitative analysis of permeability under the influence of temperature or gas pressure on a single factor. Although it provides an important theoretical basis and basis to produce models on permeability, the permeability models considering limited factors often overestimate matrix deformation's effect due to gas adsorption on fracture deformation, resulting in a certain degree of error between the permeability calculation results and the permeability obtained from the experimental data of coal creep and seepage. Furthermore, there are few studies on the permeability evolution model of matrix−fissure interaction which takes into account creep deformation, temperature factor, thermal expansion, and gas adsorption deformation.

Gas treatment in high-temperature, high-stress, and low-permeability coal seams is a coupling problem of the temperature field, gas pressure field, and coal deformation field. However, qualitative and quantitative analyses of the impact of a single factor on the permeability law are common in prior research. The permeability evolution model of matrix−crack interaction caused by creep deformation, temperature factor, as well as deformation and thermal expansion caused by gas adsorption are also taken into account, and the multifield coupling permeability evolution model is combined with the transport response equations of coal gas migration, seepage field, diffusion field, stress field, and temperature field. The multifield coupling of coal seam gas migration as well as the influence of coal seam thermal effects on gas extraction properties have been the subject of limited research.

Therefore, to examine this evolution process of coal creep deformation as well as gas seepage under multifield coupling, this paper establishes a creep model due to the effect of temperature according to analyzing the coal creep deformation evolution law under high ground temperature. To comprehend entirely the gas transport law regarding a coal body under multifield coupling, related law on the evolution of permeability due to combined effects of temperature, creep deformation, and matrix−fracture interaction is studied. Experiments and theoretical models of creep and seepage under different temperature conditions are carried out. Combined with the evolution of permeability in the experimental data, a model on permeability is formulated by determining the interplay between matrix−fracture interaction, creep deformation, and temperature.

During gas extraction in coal seams, the gas migration law is affected by many factors, especially the temperature. Based on a model of permeability depicting interplays between matrix−fracture interaction, creep deformation, and temperature, combined with coal gas migration, seepage field, diffusion field, stress field, and temperature field, a coal gas migration coupling model based on multiple fields is constructed. Based on actual mine geological conditions and coal seam condition parameters, the corresponding physical model and initial conditions are established, and we apply simulation through numerical means for analyzing the evolution law of gas migration under the influence of external factors. This paper mainly analyzes the influence of the coal seam thermal effect on gas extraction characteristics. The study of the multifield coupled model of coal seam gas migration plays an important role in comprehending the impact of elevated temperature on permeability as well as its application in gas extraction while also depicting a guiding function toward improving field gas extraction engineering technology.

https://doi.org/10.1021/acsomega.4c01706
ACS Omega 2024, 9, 22871−22891

2. EXPERIMENTAL STUDY

2.1. Creep and Seepage Experiments at Different Temperatures. The coal sample used in this research was taken from the no. 8 coal seam of Baode Coal Mine. In the coal mine, the size of the coal block was about 600 mm × 400 mm × 400 mm, and the block was sealed with plastic wrap and sent to the rock mechanics laboratory to determine the coal's basic mechanical and physical attributes. The standard sample, which measured 100 mm in height and 50 mm in diameter, was fabricated from the coal mass in adherence to the guidelines set forth by the International Society of Rock Mechanics.

The test instrument adopts a comprehensive test system, as shown in Figure 1. The test instrument can be loaded with an

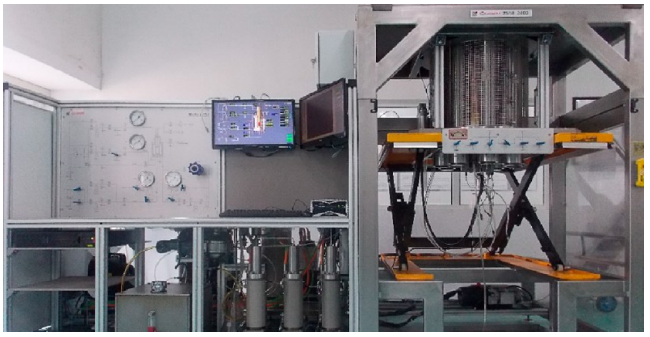

Figure 1. Comprehensive experimental system.

axial loading force of up to 200 MPa, with an axial pressure applied by hydraulic pressure and a maximum confining pressure of 100 MPa. The temperature is controlled by a separate module, and the maximum temperature applied is 200 °C. The axial and transverse deformation can be measured by two sets of strain gauges. Among them, the hydraulic servo controls the three-axis rheometer and the heating device and the strain measuring device. The temperature at which the creep and seepage experiments were performed was 25 °C.

The experimental equipment used in the experimental research institute is a comprehensive experimental system, and the specific steps of coal creep and seepage test under different temperature conditions are as follows:

(1) *Apply hydrostatic pressure.* The concurrent loading of the confining pressure and axial pressure was varied between 2 and 25 MPa, contingent upon the in situ stress state being examined at the location.
(2) *Load the axial deviating stress.* The deviating stress was increased to 30 MPa while maintaining the confining pressure at 25 MPa.
(3) *Control temperature.* While the confining and axial pressures were kept constant, the three test temperatures were set as 30, 50, and 70 °C.
(4) *Measure permeability.* The external stress state was kept unchanged, and nitrogen was injected from the upper end of the coal body while the osmotic pressure difference between the upper and lower ends was maintained at 2 MPa. When the data were relatively stable, the permeability was measured.

2.2. Experimental Results and Analysis of Creep and Seepage. To examine the osmotic evolution law during the creep deformation of coal under different temperatures, three sets of creep seepage tests at 30, 50, and 70 °C were set under a 30 MPa axial pressure and a 25 MPa confining pressure. Figure 2 provides the outcomes from the creep curve test.

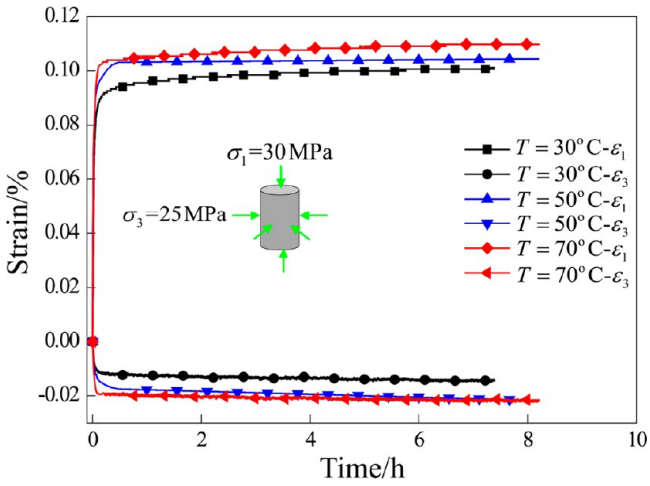

Figure 2. Creep deformation curves at different temperatures.

The data from creep tests conducted on three distinct groups at varying temperatures indicate that axial strain increases gradually alongside the temperature, as depicted in Figure 2. The lateral strain basically shows the same trend, but the difference of lateral strain is relatively small. When the temperature is 30, 50, and 70 °C, the maximum axial strain of the three groups of coal is 0.102%, 0.106%, and 0.111%, respectively, showing a trend of $\Delta\varepsilon_1^{70} > \Delta\varepsilon_1^{50} > \Delta\varepsilon_1^{30}$. As the temperature rises, the transverse creep deformation increment is different from that of axial creep deformation, and the transverse strain is −0.014%, −0.022%, and −0.021%, respectively, showing a trend of $\Delta\varepsilon_3^{50} > \Delta\varepsilon_3^{70} > \Delta\varepsilon_3^{30}$. The experimental data show that a direct correlation arises in axial creep deformation with respect to the temperature. The transverse creep deformation and axial stress have no obvious rule. It may be determined from creep deformation data of coal body under three different temperature states that thermal damage occurs inside coal body due to temperature, which degrades the coal body's mechanical attributes while leading to higher axial creep deformation.

The progressive reduction in the permeability of the coal mass during creep deformation is illustrated in Figure 3. A reduction in temperature causes a departure in the permeability of the coal body. Coal correspondingly exhibits an initial permeability of 3.95×10^{-19}, 3.31×10^{-19}, and 2.55×10^{-19} m^2 at 30, 50, and 70 °C, respectively.

According to Figure 4, with the progress of coal creep deformation, the final coal permeability changes at 30, 40, and 50 MPa axial pressure are 13.5×10^{-19}, 36.5×10^{-19}, and 3.7×10^{-19} m^2, respectively. The permeability change shows a trend of $\Delta k^{40} > \Delta k^{30} > \Delta k^{50}$. Coal permeability does not increase monotonically with axial stress due to the complexity and variation in its pore structure. However, the experimental data of coal creep and seepage show that the coal permeability progressively decreases alongside creep deformation. The analysis shows that the gas desorption ability is enhanced due to the increase of test temperature, and coal matrix expansion and deformation lead to compression of the internal pores of coal, which inhibits coal permeability. The evolution law of permeability in this process is analyzed through creep and seepage tests under different temperature conditions,

https://doi.org/10.1021/acsomega.4c01706
ACS Omega 2024, 9, 22871−22891

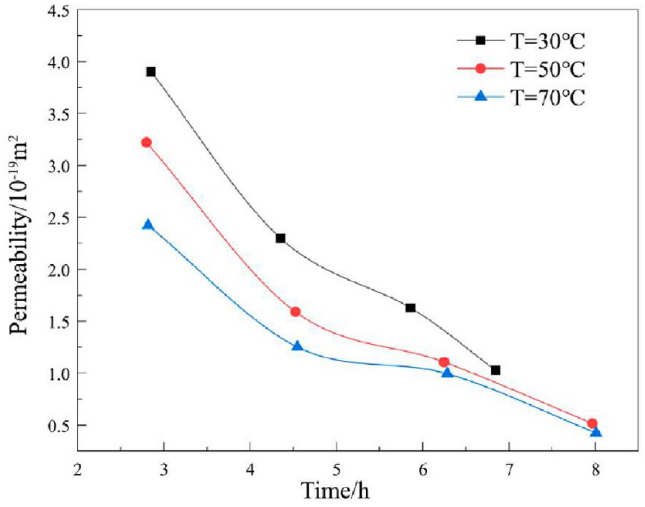

Figure 3. Permeability evolution under creep condition.

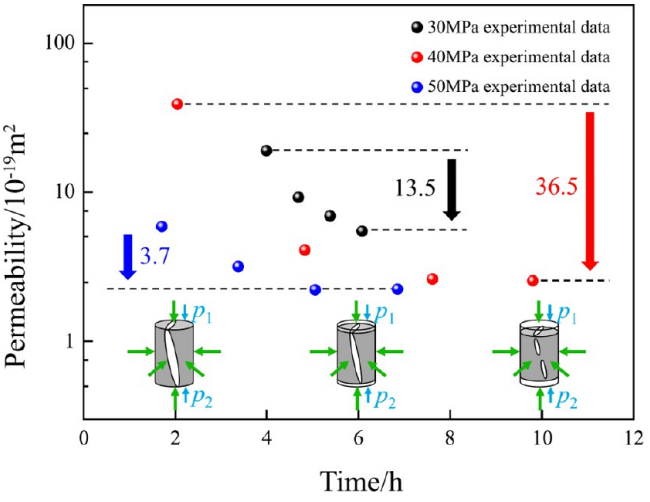

Figure 4. Permeability evolution under creep condition.

which renders an important foundation for experimenting with high-temperature mine treatment.

3. THEORETICAL MATHEMATICAL MODEL OF COAL PERMEABILITY EVOLUTION CONSIDERING TEMPERATURE

3.1. Analysis of Influence of Temperature on Fracture Opening and Porosity. Through coal creep and seepage tests based on varying temperatures, the temperature has an important influence on the evolution law of coal deformation and permeability. In order to ascertain the impact of temperature on coal pore structure and permeability, based on the theory of thermodynamics and rock mechanics, a coal porosity model under the coupled action of creep, thermal, and seepage is established from the perspective of thermal expansion deformation, creep deformation, and gas adsorption.

Coal deformation and fissure cracking often have an impact on coal fracture and porosity, which are significantly influenced by its temperature and stress state. To probe the effect of temperature and creep deformation on the coal pore structure, a coal crack opening evolution model was generated, as depicted by Figure 5.

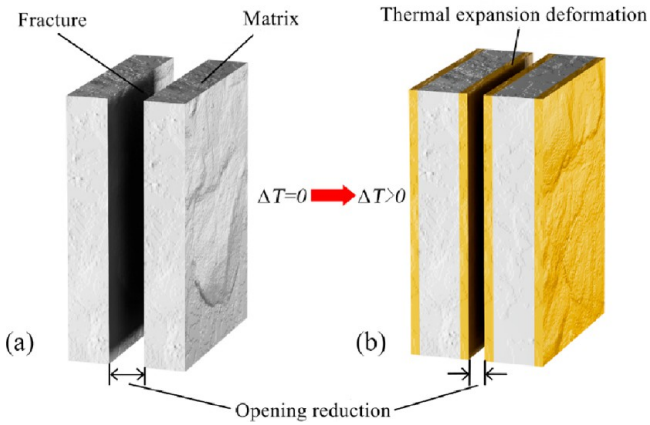

Figure 5. Evolution of fracture aperture when subjected to deformation via thermal expansion. (a) Matrix model of coal fissure. (b) Thermal expansion affects matrix evolution of coal fissure.

Coal matrix deformation is predominantly attributable to external stresses, the creep deformation, and the thermal expansion deformation. Under constant load, as the temperature increases, the coal matrix undergoes more deformation, resulting in a contraction of its crack, which leads to a decrease of the coal porosity. The formula for porosity of coal is[24]

$$\phi = \frac{V_f}{V_b} = \frac{V_{f0} - \Delta V_T}{V_{b0} + \Delta V_T} = \frac{(V_{f0} - \Delta V_T)/V_{b0}}{(V_{b0} + \Delta V_T)/V_{b0}} = \frac{\phi_0 - \Delta\varepsilon_T}{1 + \Delta\varepsilon_T} \quad (1)$$

in which

$$\Delta\varepsilon_T = \alpha_T \Delta T \quad (2)$$

where V_f represents the coal body's pore and crack volume, ΔV_T denotes the increment in volume due to coal matrix deformation via thermal expansion, V_b signifies coal matrix volume, α_T represents the coal matrix coefficient for thermal expansion (in K^{-1}), $\Delta\varepsilon_T$ denotes strain coming from such thermal expansion, $\Delta T = T - T_0$ is the temperature increment (in °C), and T_0 is 25 °C.

According to eq 1, at higher temperature and a coefficient of thermal expansion of 1×10^{-4} K^{-1}, the porosity of coal exhibits a progressive decline from its initial value of 5%. When the thermal expansion coefficient is 5×10^{-4} K^{-1} and 1×10^{-3} K^{-1}, the coal permeability decline increases. It shows that as the coefficient of thermal expansion increases, the reduction in coal permeability becomes more pronounced. The thermal expansion evolution trend of the porosity is shown in Figure 6.

To facilitate the calculation, this section focuses on the effect of temperature on the viscoelastic deformation phase ($\Delta\varepsilon^e_{vp} = 0$). The constitutive equation for the viscoelastic deformation of the heat−force coupled fractional creep model can be expressed as[15]

$$\varepsilon(t) = \frac{\sigma}{E_e(T)} + \frac{\sigma}{E_{ve}(T)}\left[1 - E_{\gamma,1}\left(-\frac{E_{ve}(T)}{\eta^{\gamma}_{ve}(T)}t^{\gamma}\right)\right] \quad (3)$$

Equation 3 analyzes the viscoelastic deformation of the coal body under different temperature conditions. The creep deformation law under different temperature conditions is shown in Figure 7. This figure shows that the creep deformation of the coal body gradually increases with the growth of time, and elevated temperatures result in an

https://doi.org/10.1021/acsomega.4c01706
ACS Omega 2024, 9, 22871−22891

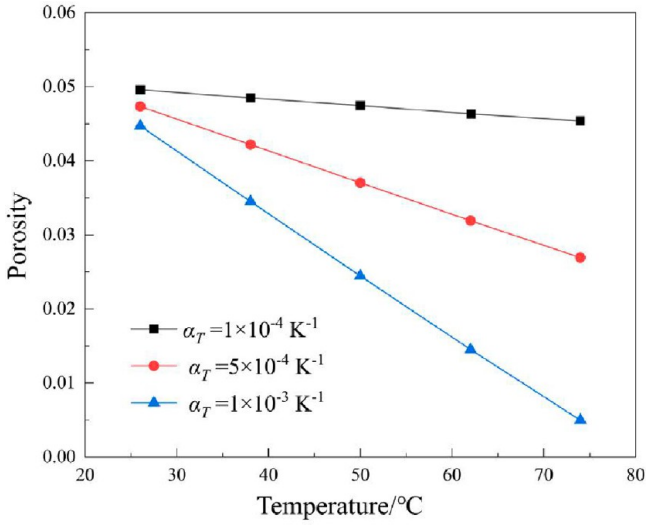

Figure 6. Porosity evolution under thermal expansion deformation.

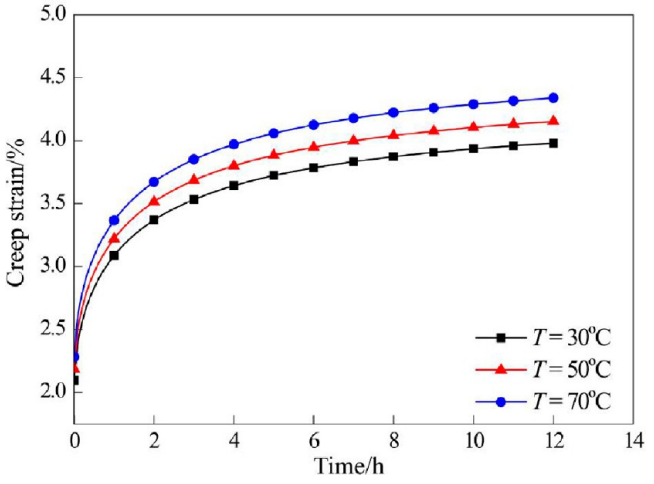

Figure 7. Creep deformation under different temperatures.

accelerated growth of creep deformation. According to the evolution law of creep deformation, temperature's effect on creep deformation also exists for a long time, that is, the temperature continuously affects the deformation of the creep. $\varepsilon(t)$ represents the effect of temperature on the viscoelastic deformation phase; σ denotes stress, MPa; $E_e(T)$ signifies the elastic modulus that takes into account the change in temperature, GPa; $E_{ve}(T)$ represents is the elastic modulus of the spring body considering the influence of temperature,GPa; η^{γ}_{ve} denotes the viscosity coefficient of Abel pot considering the influence of temperature,GPa·h γ.

Numerous investigations have discovered that the presence of gas within coal deforms the coal matrix. The pores of the coal body contain gas in two states, adsorbed and free, with the adsorbed state being the more prevalent. At constant temperature, the calculation equation of coal matrix is as follows:[24]

$$\Delta\varepsilon_{ad} = \varepsilon_L\left(\frac{p}{p + p_L} - \frac{p_0}{p_0 + p_L}\right) \tag{4}$$

where p_L is the gas Langmuir adsorption pressure constant (in MPa), p is the gas pressure (in MPa), p_0 is the initial gas pressure (in MPa), and ε_L is the gas Langmuir adsorption volume strain.

During the mining of coal, the working face is often not in a constant-temperature state, and the calculation equation of coal matrix in a non-constant-temperature state is as follows:[25]

$$\Delta\varepsilon^{T}_{ad} = \varepsilon_L\left[\frac{p}{p + p_L}\exp\left(-\frac{c_2\Delta T}{1 + c_1 p}\right) - \frac{p_0}{p_0 + p_L}\right] \tag{5}$$

where c_1 is the the gas adsorption pressure coefficient (in MPa^{-1}) and c_2 is the temperature coefficient (in K^{-1}).

Disregarding the impact of other variables on the deformation of the coal body matrix, the effect of the adsorption deformation law on the change in pore structure of the coal body is examined. The adsorption expansion deformation will reduce the opening of the coal crack and then

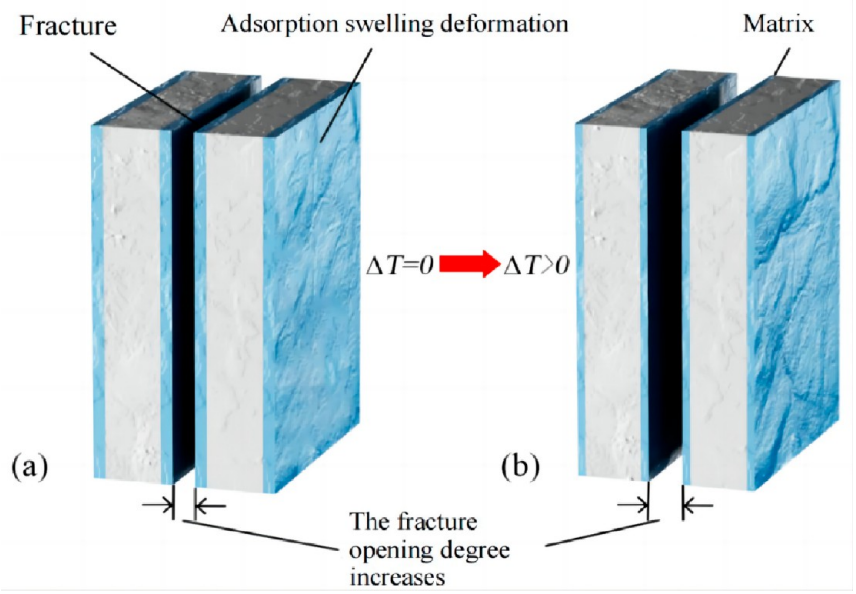

Figure 8. Fracture aperture evolution under adsorption swelling deformation.

https://doi.org/10.1021/acsomega.4c01706
ACS Omega 2024, 9, 22871−22891

reduce the porosity. When the temperature increases, the gas desorption ability increases, which will increase the fissure opening and the porosity. Deformation's influence via adsorption expansion on the crack opening is shown in Figure 8.

Considering only the adsorption deformation effect on coal porosity, the porosity is calculated as follows:[26]

$$\phi = \frac{V_f}{V_b} = \frac{V_{f0} + \Delta V_{ad}}{V_{b0} - \Delta V_{ad}} = \frac{(V_{f0} + \Delta V_{ad})/V_{b0}}{(V_{b0} - \Delta V_{ad})/V_{b0}} = \frac{\phi_0 + \Delta\varepsilon_{ad}^T}{1 - \Delta\varepsilon_{ad}^T} \quad (6)$$

where ΔV_{ad} is the volume increment caused by gas adsorption.

As gas pressure rises, coal porosity increases, as illustrated in Figure 9. Due to the influence of temperature, the higher the temperature, the higher is the porosity, showing the positive correlation between temperature and porosity. The study shows that as the temperature rises, so does the capacity for gas desorption, which reduces the coal matrix's gas-adsorption-induced expansion deformation.

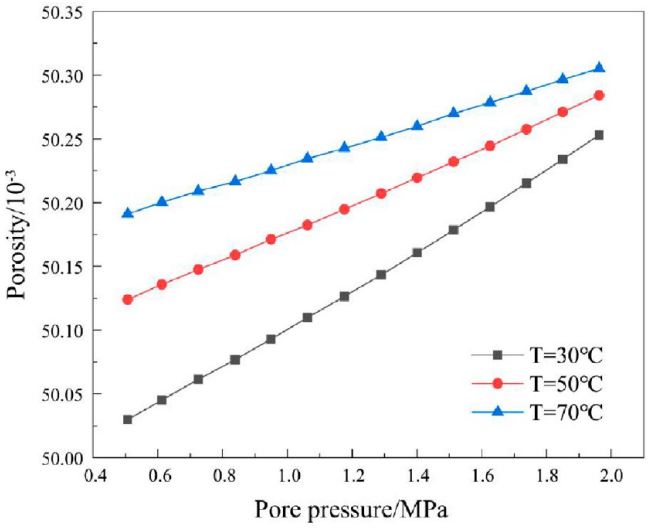

Figure 9. Porosity evolution under adsorption swelling deformation.

3.2. Matrix−Fracture Interaction Model Based on Gas Adsorption and Desorption and Thermal Expansion Deformation. Based on the principle of thermodynamics and permeability theory, the last section explored temperature's effect on the coal matrix deformation from the perspectives of thermal expansion deformation, creep deformation, and gas adsorption, thus affecting the coal body's pore structure changes. The coal body's creep deformation is several times greater than deformations due to gas adsorption or thermal expansion, according to experimental data. Considering the intricate nature of the coal body's internal pore structure, the influence of coal matrix deformation as a result of the external environment on the porosity of the coal body cannot be directly superimposed, and the interaction between the fissure and the coal matrix should also be considered.

In order to explore the interaction between the coal matrix and the fissure, it is assumed that there is a matrix bridge existing in the coal fissure (solid filling material in the fissure), as shown in Figure 10b,c, because the influence of coal deformation on the crack deformation is reduced. In addition to altering the coal body's overall volume, the gas adsorption and expansion deformation also affect crack opening and volume, as shown in Figure 10f. When the temperature is constant, the coal matrix deformation is mainly caused by gas adsorption and expansion deformation, as shown in Figure 10e. When the temperature rises, the thermal expansion deformation and gas adsorption expansion deformation comprise coal matrix deformation. Among them, the temperature increase will increase the gas desorption capacity, and as Figure 10g reflects, this reduces the deformation of gas adsorption caused by an increase in the temperature.

When a coal body matrix undergoes volume expansion deformation, the deformation consists predominantly of two constituent elements: crack deformation and coal body deformation. A parameter is defined to characterize the degree of coal matrix−cleft interaction, that is, the coupling internal expansion coefficient f_{ST} $(0 < f_{ST} < 1)$. This parameter is the ratio of fissure deformation and matrix deformation caused by gas adsorption and thermal expansion. Its expression is as follows:[26]

$$\Delta V_m^{ST} = \Delta V_b^{ST} + \Delta V_f^{ST} \quad (7)$$

$$\Delta V_f^{ST} = f_{ST}\Delta V_m^{ST}, \quad \Delta V_b^{ST} = (1 - f_{ST})\Delta V_m^{ST} \quad (8)$$

The strain increase in the volume of the crack and coal, which is the result of thermal expansion deformation and gas adsorption combined, can be mathematically represented as follows:[25]

$$\Delta\varepsilon_f^{ST} = \frac{\Delta V_f^{ST}}{V_f} = \frac{f_{ST}\Delta V_m^{ST}}{V_f} = \left(\frac{1 - \phi}{\phi}\right) f_{ST}\Delta\varepsilon_m^{ST} \quad (9)$$

$$\Delta\varepsilon_b^{ST} = \frac{\Delta V_b^{ST}}{V_b} = \frac{(1 - f_{ST})\Delta V_m^{ST}}{V_b} = (1 - \phi)(1 - f_{ST})\Delta\varepsilon_m^{ST} \quad (10)$$

$$\Delta\varepsilon_m^{ST} = \Delta\varepsilon_{ad}^T + \Delta\varepsilon_T = \varepsilon_L\left[\frac{p}{p + p_L}\exp\left(-\frac{c_2\Delta T}{1 + c_1 p}\right) - \frac{p_0}{p_0 + p_L}\right] + \alpha_T\Delta T \quad (11)$$

where $\Delta\varepsilon_f^{ST}$ is the fracture volume strain increment, $\Delta\varepsilon_b^{ST}$ is the volume strain increment of coal, and $\Delta\varepsilon_m^{ST}$ is the volume strain increment of the coal matrix.

Under constant external load, an improved permeability model is developed by incorporating temperature as a factor in addition to the matrix−fracture interaction and creep deformation components, that is, the permeability model under multifield coupling of creep−thermal−seepage. The specific expression of the model is as follows:[15]

$$\frac{k}{k_0} = \left[1 + \underbrace{\frac{\alpha}{\phi_0}(\Delta\varepsilon_e^T + \Delta\varepsilon_{ve}^T)}_{\substack{\text{creep}\\ \text{temperature}}} + \underbrace{\frac{f_{ST}}{\phi_0}(\Delta\varepsilon_m^{ST})}_{\substack{\text{matrix−fracture interaction}\\ \text{temperature}}}\right]^3 \quad (12)$$

where $\Delta\varepsilon_e^T$ is the effective elastic volume strain increment, α is the Biot coefficient, and $\Delta\varepsilon_{ve}^T$ is the effective viscoelastic volume strain increment.

Based on the above derivation, combining eq 8, eq 9, and eq 12 with the coal permeability model (MCT model) considering temperature influence, creep deformation, and

https://doi.org/10.1021/acsomega.4c01706
ACS Omega 2024, 9, 22871−22891

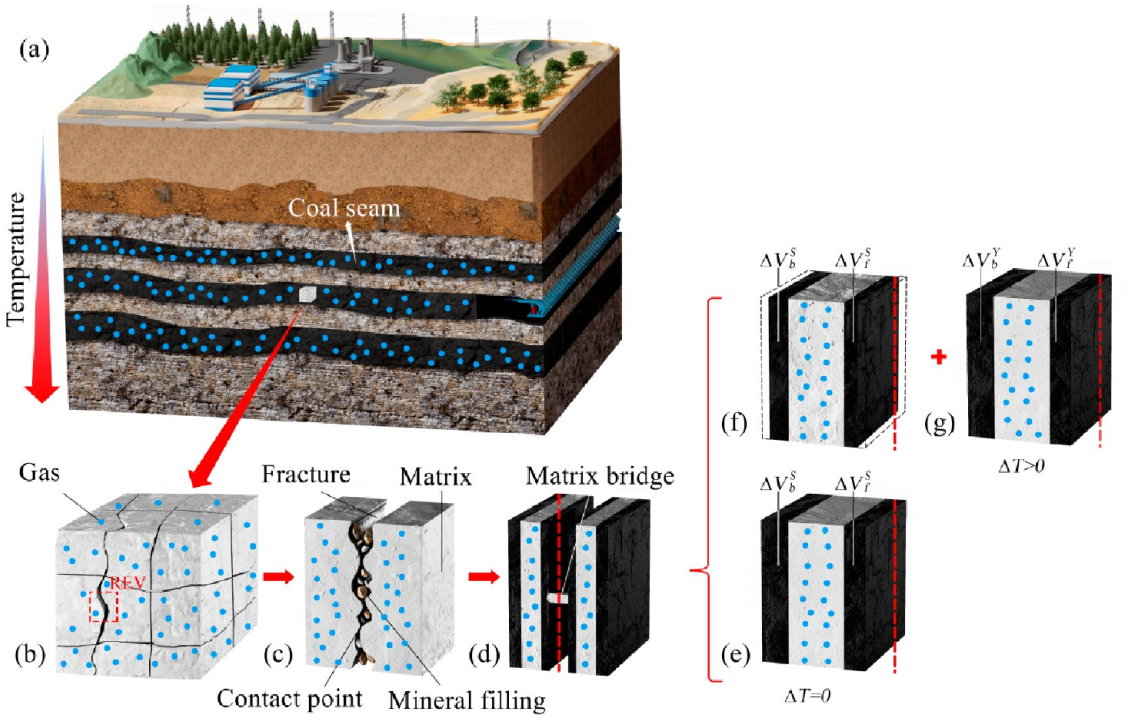

Figure 10. Schematic diagram of actual mining. (a) 3D map of coal seam mining. (b) Coal structure mode(REV)l. (c) Fracture and matrix. (d) Matrix−-crack interaction model. (e, f) Matrix adsorption deformation. (g) Matrix thermal expansion deformation.

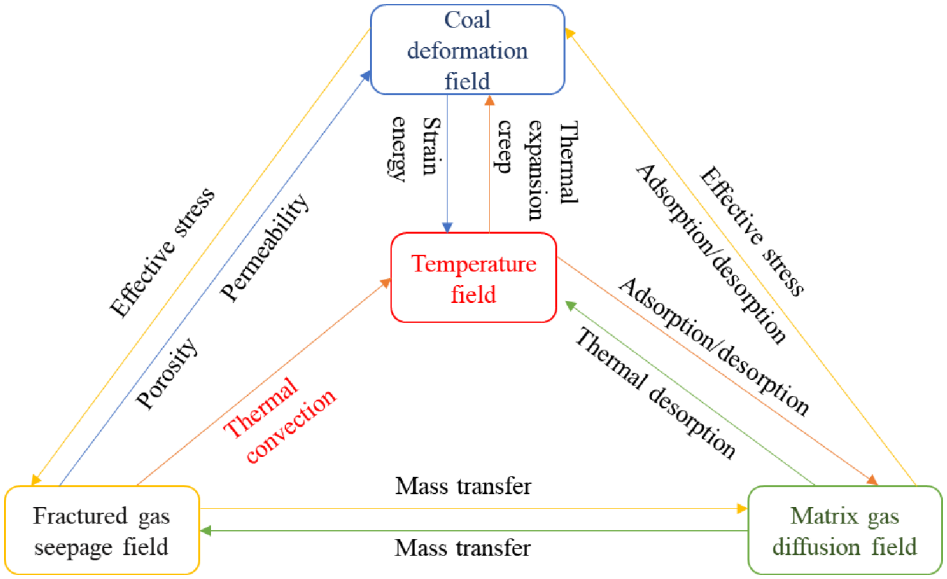

Figure 11. Multifield coupling relation.

matrix−cleft interaction, the permeability model expression is as follows:

$$\frac{k}{k_0} = \left(1 + \frac{\alpha}{\phi_0}(\Delta\varepsilon_e^T + \Delta\varepsilon_{ve}^T) + \frac{f_{ST}}{\phi_0}\left\{\varepsilon_L\left[\frac{p}{p + p_L}\exp\left(-\frac{c_2\Delta T}{1 + c_1 p}\right) - \frac{p_0}{p_0 + p_L}\right] + \alpha_T\Delta T\right\}\right)^3 \quad (13)$$

where k_0 is the initial permeability (in m^2).

4. NUMERICAL SIMULATION ANALYSIS

4.1. Multiphysical Field Coupling Model of Coal Body. The control equations describing gas migration in coal are established by using the seepage field, diffusion field, temperature field, coal constitutive equation, and permeability model, and every physical field exhibits coupling.[27−29] The equations of the seepage field and diffusion field describe two forms of gas seepage in cracks and diffusion in pores.[30,31] Temperature's effect on gas desorption and adsorption heat, heat convection, free gas, and coal deformation is considered in the governing equation of the temperature field.[32,33] In contrast to the constitutive equation, which accounts for stress

https://doi.org/10.1021/acsomega.4c01706
ACS Omega 2024, 9, 22871−22891

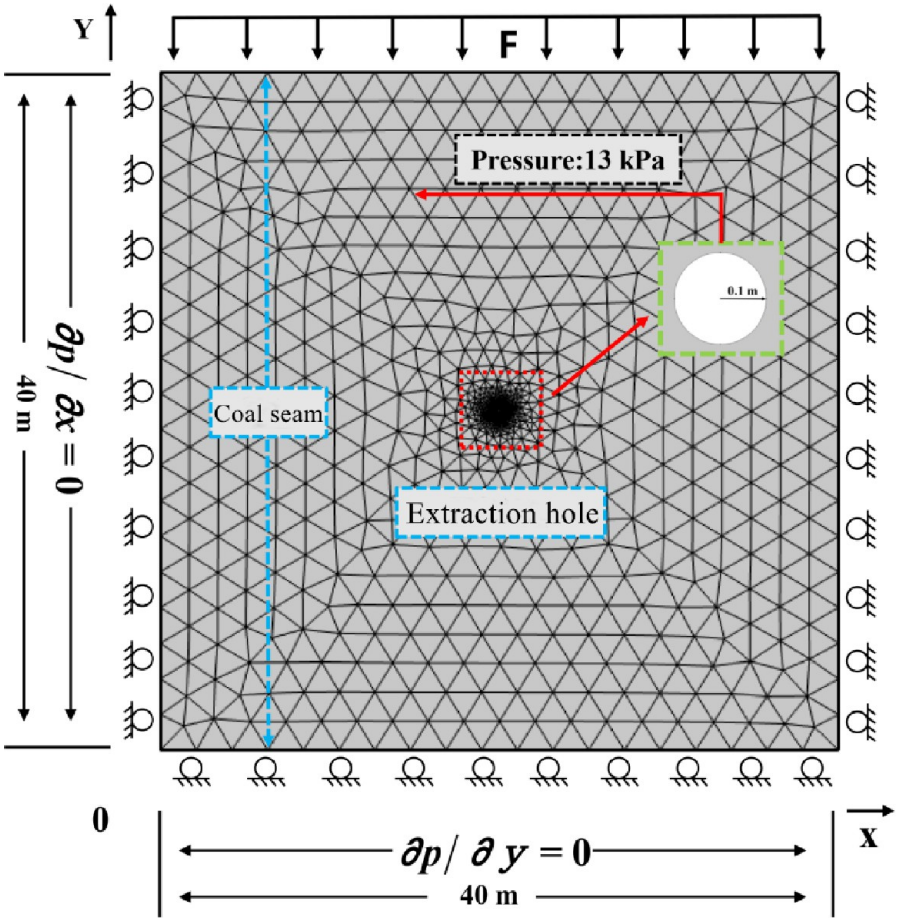

Figure 12. Physical model and boundary conditions of coal.

and temperature-induced deformation, the permeability model also incorporates the influences of creep, gas pressure, and temperature on permeability.[31] The multiphysical field coupling relationship is shown in Figure 11.

diffusion field governing equation:[1]

$$\frac{\partial}{\partial t}\left[\frac{V_L p_m}{p_m + p_L}\exp\left(\frac{-c_1(T - T_{ref})}{1 + c_2 p_m}\right)\frac{M_c}{V_M}\rho_c + \phi_m\frac{M_c}{RT}p_m\right] = \frac{1}{\tau}\frac{M_c}{RT}(p_m - p_f)$$

governing equation of seepage field:[34]

$$p_f\frac{\partial \phi_f}{\partial t} + \phi_f\frac{\partial p_f}{\partial t} - \nabla\left(p_f\frac{k}{\mu}\nabla p_f\right) = \frac{1}{\tau}(p_m - p_f)(1 - \phi_f)$$

coal constitutive equation:[25]

$$Gu_{i,jj} + \frac{G}{1 - 2v}u_{j,ji} - \beta_f p_{f,i} - \beta_m p_{m,i} - K\frac{\varepsilon_L p_m}{p_m + p_L}\exp\left[-\frac{c_1(T - T_{ref})}{1 + c_2 p_m}\right] - K\alpha_T\Delta T + F_i = 0$$

temperature field governing equation:[22,27]

$$(\rho C)_M\frac{\partial T}{\partial t} + TK\alpha_T\frac{\partial \varepsilon_v}{\partial t} = \lambda_M\nabla^2 T + \frac{\rho_g p_m T_a C_g}{p_a T}\frac{k}{\mu}\nabla p\nabla T$$

permeability model:

$$\frac{k}{k_0} = \left(1 + \frac{\alpha}{\phi_0}(\Delta\varepsilon_e^T + \Delta\varepsilon_{ve}^T) + \frac{f_{ST}}{\phi_0}\left\{\varepsilon_L\left[\frac{p_m}{p_m + P_L}\exp\left(-\frac{c_2\Delta T}{1 + c_1 p_m}\right) - \frac{p_0}{p_0 + P_L}\right] + \alpha_T\Delta T\right\}\right)^3$$

4.2. Physical Model Construction and Parameter Selection. In order to fully, truly, and effectively consider the influence characteristics of the MCT permeability evolution model on gas extraction law, first an establishment of a credible coal physical model is imperative. This model is determined by actual coal seam conditions and the characteristics of the numerical model. The three-dimensional coal model is simplified into a two-dimensional coal model without affecting the simulation results.

4.2.1. Physical Model Construction and Boundary Conditions. In this paper, COMSOL Multiphysics coupled software for numerical simulation was used to calculate migration of gas in coal. The two-dimensional physical model sets a square coal seam with a side length of 40 m and a drilling scale of 0.1 m. According to the actual stress

https://doi.org/10.1021/acsomega.4c01706
ACS Omega 2024, 9, 22871−22891

conditions of the coal seam, we established the coal seam's deformation field's boundary conditions. The roller boundaries are established on the physical model's left and right sides. The coal seam is covered with constant ground stress, which can be considered as the constant load boundary, and the fixed boundary of the model is located at its base. In the gas flow field, the scale of the borehole is much smaller than that of the coal seam, and since extraction from the borehole has little impact on the boundary surrounding the coal vein, zero flow boundaries are established on all four sides of the model.[27,35] Figure 12 illustrates the coal seam's boundary conditions and physical model.

4.2.2. Parameter Selection. According to the above section, some of the coal parameters were determined, and the measured parameters were applied to the model for calculation. Except for the parameters that affect creep, which need to be set separately, the remaining parameters were obtained from the literature of other scholars. A summary table of fixed parameters is shown in Table 1.[36−38]

Table 1. Summary of Numerical Simulation Fixed Parameters

parameter	numerical value
initial permeability, k_0	4.935×10^{-16} m^2
adsorption time, τ	10 days
coal body density, ρ_c	1.25 ton/m^3
initial porosity, ϕ_{f0}	0.005
standard gas volume, V_M	22.4 L/mol
molar mass of methane, M	16 g/mol
gas constant, R	8.314 J^{-1}·mol^{-1}·K^{-1}
initial gas pressure, P_0	0.8 MPa
gas dynamic viscosity, μ	1.08×10^{-5} Pa·s
gas density, ρ_g	0.717 kg/m^3
gas Langmuir volume constant, V_L	0.02 m^3/kg
gas Langmuir pressure constant, P_L	10 MPa
gas Langmuir strain constant, ε_L	0.002
modulus of elasticity, E	2713 MPa
initial coal seam temperature, T_0	310 K
gas desorption reference temperature, T_{ref}	300 K
thermal coefficient of the gas temperature adsorption, c_1	0.028 K^{-1}
thermal coefficient of the gas pressure adsorption, c_2	0.068 MPa^{-1}
coefficient of expansion due to heat, α_T	0.0001 K^{-1}
coal-matrix elastic modulus, E_m	8139 MPa
Poisson ratio, υ	0.28
porosity, ϕ_{m0}	0.00091
gas thermal conductivity, λ_c	0.031 W·m^{-1}·K^{-1}
thermal conductivity of the coal body, λ_s	0.191 W·m^{-1}·K^{-1}
gas adsorption heat, q_{st}	33.4 J/mol
specific heat capacity of coal skeleton, C_s	1350 J·kg^{-1}·K^{-1}
specific heat capacity of gas pressure, C_g	2160 J·kg^{-1}·K^{-1}

4.3. Analysis of Influence of Thermal Effect on Gas Extraction Characteristics. To compare the gas migration law under varying initial coal seam temperatures, some key parameters include the initial coal seam temperature, initial coal seam gas pressure, and initial coal seam permeability, as shown in Table 2.

4.3.1. Time-Varying Mechanism of Temperature Field. To probe the temperature field's time-varying mechanism at different initial coal seam temperatures, the MCT permeability evolution model constructed above is used to calculate the gas extraction time to 1000 days and extract the temperature evolution cloud maps of four different time nodes of 10, 100, 500, and 1000 days, respectively, as shown in Figures 13, 14, and 15. Accordingly, at the same initial seam temperature, the temperature around the drilling hole decreases significantly, the temperature change radius increases, and the part of the coal seam distant to the center of the drill experiences less temperature effect and the temperature decreases slowly. With rising temperature of the coal seam, the temperature field evolution is similar, and the corresponding temperature increases as the initial seam temperature increases. Considering initial and boundary condition constraints, it is difficult to intuitively observe the more subtle changes of the temperature field only from the temperature field evolution cloud map.

Table 2. Partial Parameter Table

parameter	numerical value
initial coal seam temperature	30, 50, 70 °C
initial coal seam gas pressure	0.8 MPa
initial coal seam permeability	4.935×10^{-16} m^2

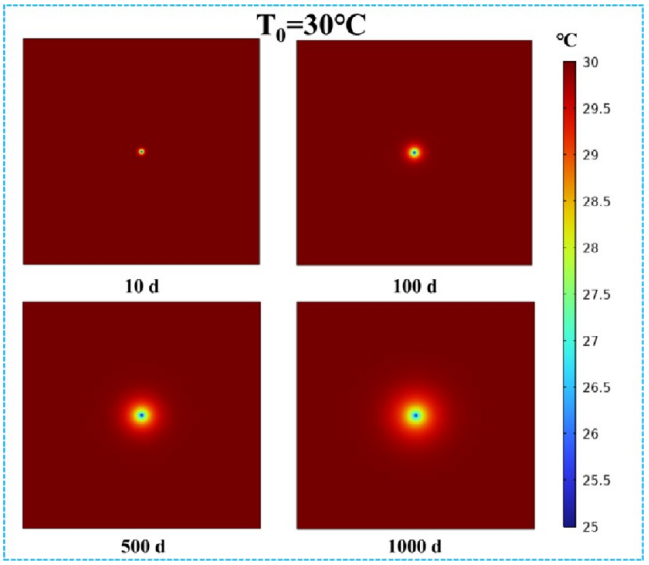

Figure 13. Temperature field evolution at different times when the initial coal seam temperature is 30 °C.

4.3.2. Gas Pressure Field Distribution and Evolution. Figures 16, 17, and 18 are the cloud maps of gas pressure field evolution considering varying times of extraction under preliminary temperatures of coal seam of 30, 50, and 70 °C, respectively. Under the premise of a different initial coal seam temperature, the extraction time increase enables a progressive decrease in gas pressure, and the higher the initial coal seam temperature, the faster the pressure drops. This is because a greater initial coal seam temperature enables a more conducive desorption of gas, and the free gas flow along the pressure gradient is higher; the higher the temperature of the coal seam, the larger is the permeability, so there is a greater temperature alongside a change in pressure in the coal seam.

5. RESULTS ANALYSIS

5.1. Analysis of Time-Varying Mechanism of Temperature Field. In order to observe the effect of the coal seam's preliminary temperature on the temperature field's evolution

https://doi.org/10.1021/acsomega.4c01706
ACS Omega 2024, 9, 22871−22891

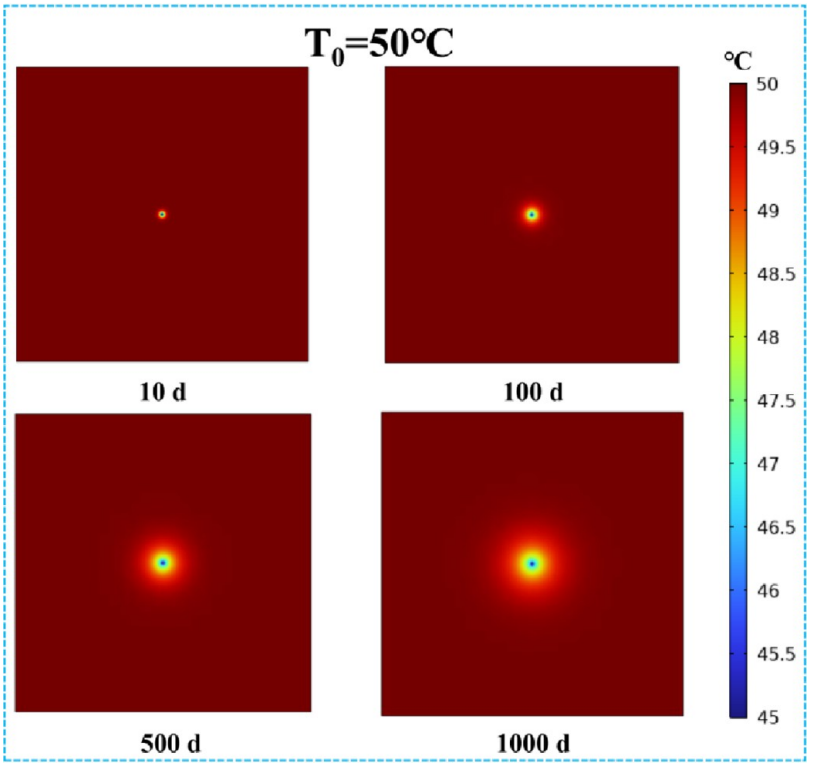

Figure 14. Temperature field evolution at different times when the initial coal seam temperature is 50 °C.

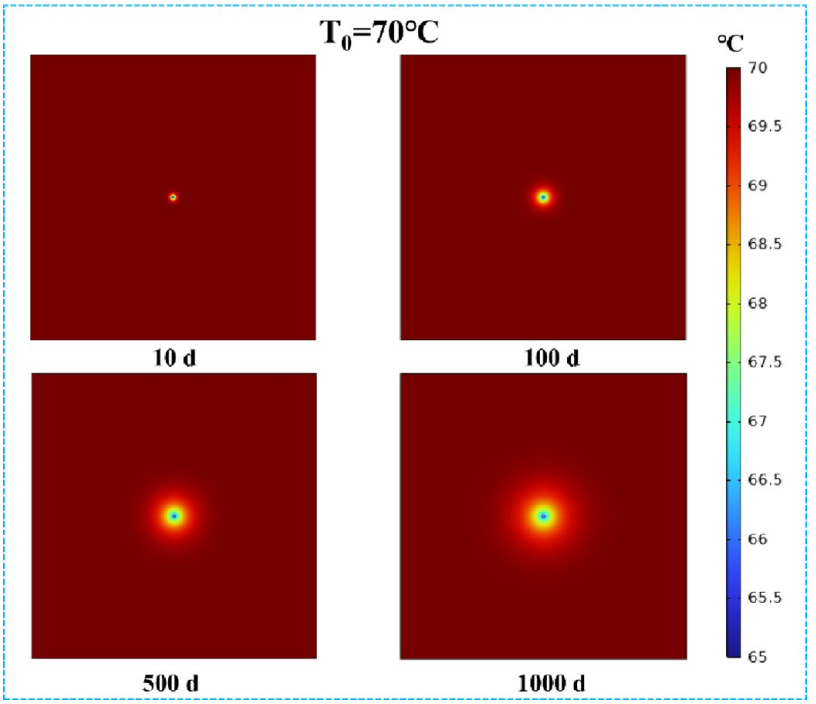

Figure 15. Temperature field evolution at different times when the initial coal seam temperature is 70 °C.

more intuitively, the temperature evolution data from the drilling hole to the two ends of the coal seam at different temperatures are extracted, respectively, and the underlying mechanism regarding initial temperature is compared and analyzed by setting different extraction times (10, 100, 500, and 1000 days), as shown in Figure 19. It can be intuitively found from the figure that regardless of the initial coal seam temperature, the far coal seam's temperature is significantly greater than that near the drilling hole. However, at the same extraction time, the trend of temperature change is smaller at a distance from the borehole, and the temperature of the coal seam drops slowly. The radius of temperature change increases in proportion to the initial temperature of the coal seam. The coal seam's gas adsorption capacity diminishes with increasing temperature, while a large amount of methane is transformed to the free state from an adsorbed one, which increases the

https://doi.org/10.1021/acsomega.4c01706
ACS Omega 2024, 9, 22871−22891

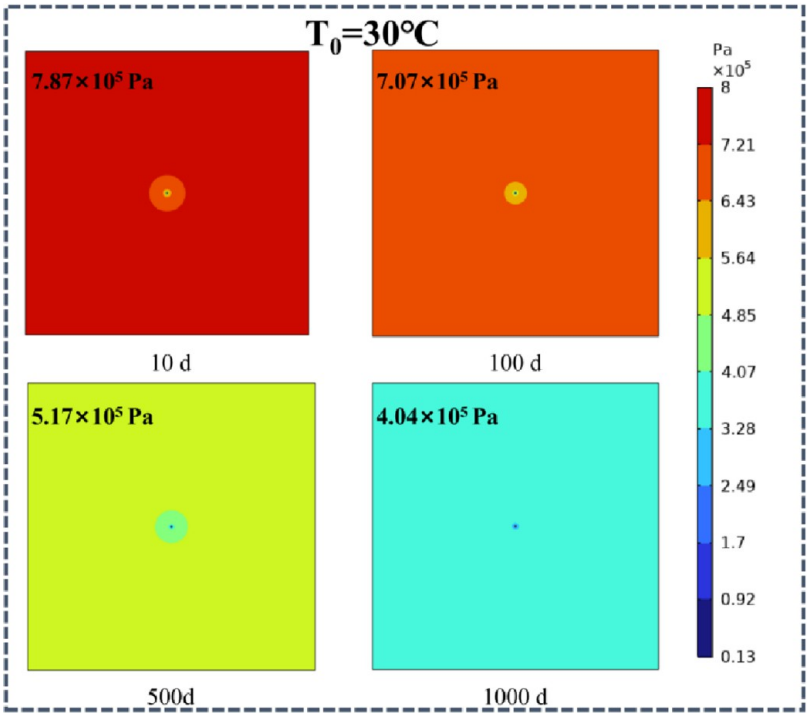

Figure 16. Evolution of the pressure field at different times when the initial coal seam temperature is 30 °C.

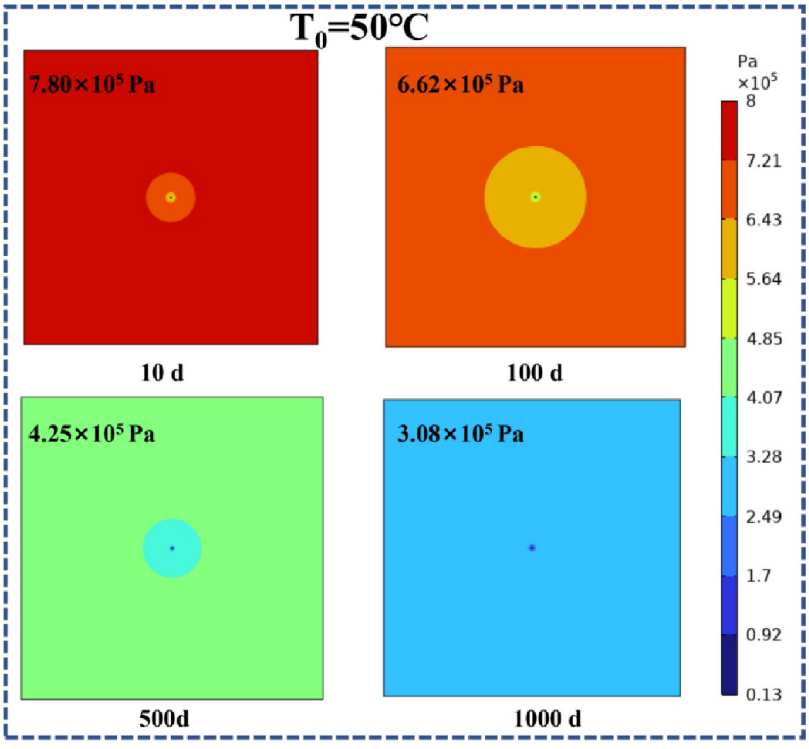

Figure 17. Evolution of the pressure field at different times when the initial coal seam temperature is 50 °C.

pressure gradient between the coal seam and the borehole, promotes the gas migration in the fissure system, and enables the far coal seam to undergo desorption earlier and faster, resulting in the trend of increasing the temperature influence radius. Significant heat can be removed by the free gas, which accelerates the rate of temperature decline in the coal seam. In addition, as the distance from the borehole decreases, the temperature change increases. A decrease in distance from the borehole results in a reduction in temperature variation, which is typically constant. This is because as extraction time progresses, both the temperature variation and the gas desorption volume of the coal seam in close proximity to the borehole increase. The temperature difference diminishes as the quantity of gas desorption in the coal seam distant from the borehole decreases. With rising time of extraction, gas adsorption and desorption will tend to an equilibrium state,

https://doi.org/10.1021/acsomega.4c01706
ACS Omega 2024, 9, 22871−22891

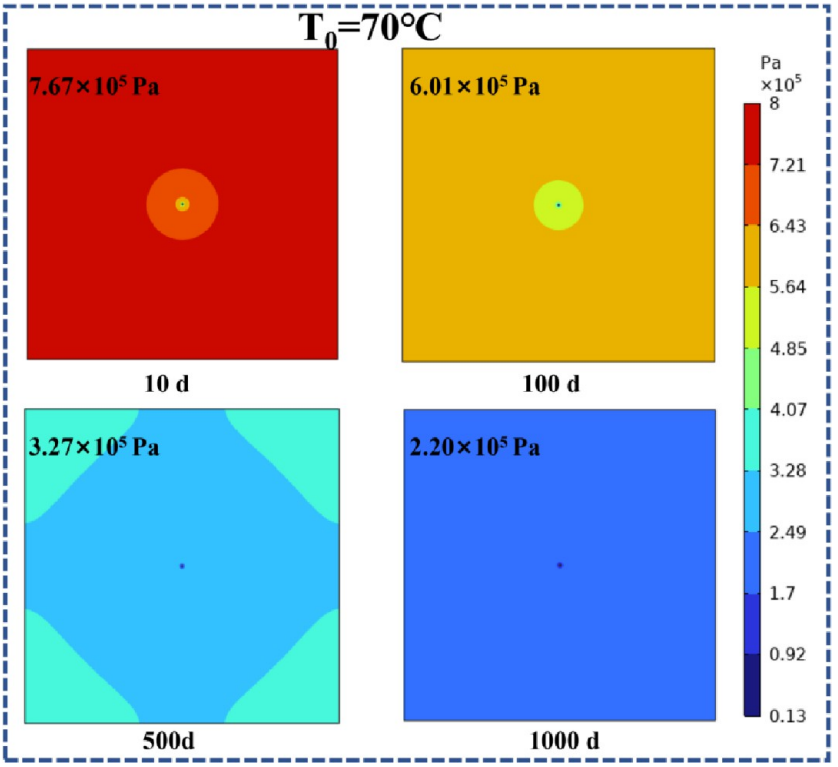

Figure 18. Evolution of the pressure field at different times when the initial coal seam temperature is 70 °C.

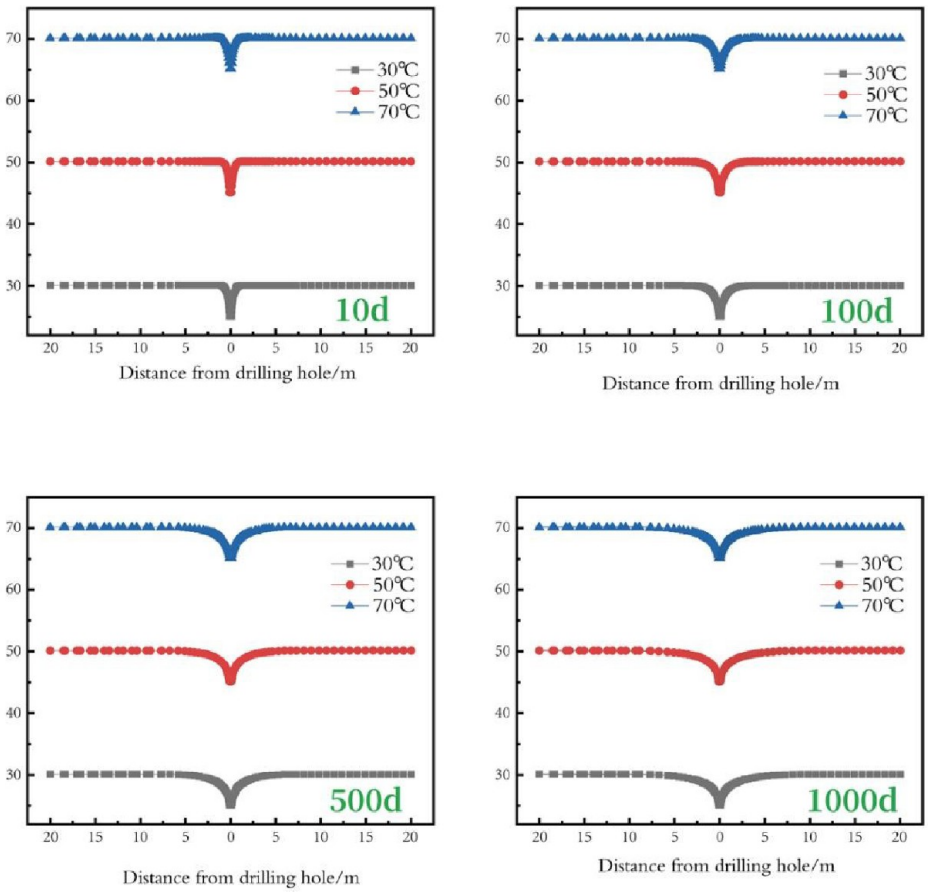

Figure 19. Evolution of temperature with distance from the borehole under different extraction times.

https://doi.org/10.1021/acsomega.4c01706
ACS Omega 2024, 9, 22871−22891

and the temperature field will also tend to be stable. Meanwhile, with the passage of extraction time, no matter how the initial coal seam temperature changes, the temperature curve becomes smoother and smoother. This indicates that the influence of the temperature field is wider. This can be attributed to the combined action of gas adsorption and desorption and gas migration. Desorption initially takes place in the vicinity of the borehole, and as the extraction time prolongs, the desorption range expands while the temperature of the succeeding coal seam diminishes.

By observing the temperature change curve at the distance of 2 m from the borehole, as described in Figure 20, under any initial coal seam temperature condition, the temperature at this distance presents a downward trend, and the rate of decline presents a trend of first fast and then slow. This is because in the early stage of gas extraction, gas desorption occurs first in the coal body near the borehole, which absorbs more heat and causes the coal body temperature within the borehole's vicinity to drop rapidly. During gas extraction at the middle and late stages, the coal body's gas proximate to the drilling hole is nearly at a state of complete desorption, and the heat taken away by gas desorption is obviously less than that in the early stage of extraction.

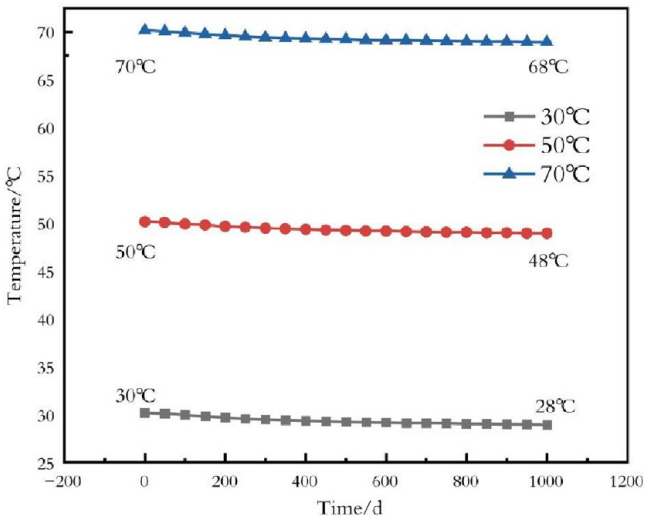

Figure 20. Time variation rule of temperature 2 m away from the borehole.

As the initial coal seam temperature during the gas extraction process increases, the disparity between the coal seam temperature and the initial temperature becomes more pronounced, as illustrated in Figure 21. This is because as the initial coal seam temperature rises, the desorption amount of gas at the same extraction time also increases, and a large amount of heat flows out of the coal seam with gas desorption, enabling a higher degree of temperature drop. At the same time, it can be found that the temperature drop degree at 2 m away from the drilling hole is significantly higher than that at 4 m away from the drilling hole.

5.2. Response Characteristics of Creep to Temperature. Creep deformation is highly dependent on the temperature and time. To probe creep deformation's association with temperature, the multiphysics field model constructed above is used to extract the creep deformation change data with time under different initial coal seam temperatures with a fixed extraction time of 1000 days, which is plotted in Figure 22. Figure 22 illustrates that as the gas extraction progression yields, the creep deformation degree is always increasing. Moreover, coal seam creep intensifies when the initial temperature of the coal seam rises. This trend indicates that the coal seam temperature is a substantial determinant to its creep degree. With the time of extraction being constant, the coal seam with high initial temperature is obviously higher than the coal seam with low initial temperature. This is because as gas extraction progresses, the coal seam temperature evolution law indicates a diminishing tendency; meanwhile, a greater initial temperature of the coal seam indicates that the decreasing trend of temperature becomes more pronounced. Therefore, the degree of creep deformation shows an obvious increasing trend on the time scale. In addition, by observing the creep deformation rules at different monitoring points, it can be found that the creep deformation of coal near the borehole (2 m) is greater than that of coal far away (19 m).

In this case, the coal temperature near the borehole changes greatly, and the corresponding creep deformation is more significant under the same extraction time. The evolution law of the creep deformation rate at different monitoring points can also be clearly seen from Figure 23. Under any initial temperature conditions, the creep rate at any monitoring point showed a downward trend. The coal body gas desorption near the borehole absorbs more heat, and the heat carried away by the free gas flow results in a large and fast change of coal body

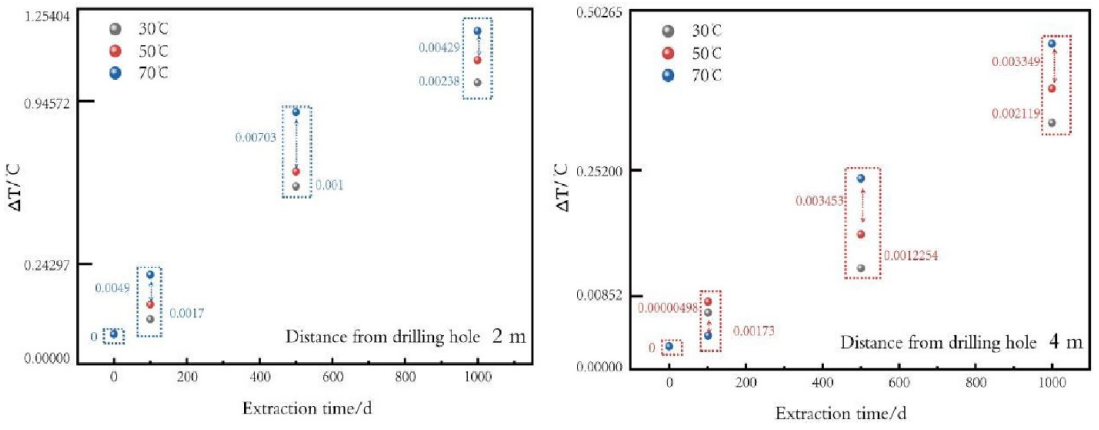

Figure 21. Temperature difference at different monitoring points under different reservoir temperatures.

https://doi.org/10.1021/acsomega.4c01706
ACS Omega 2024, 9, 22871−22891

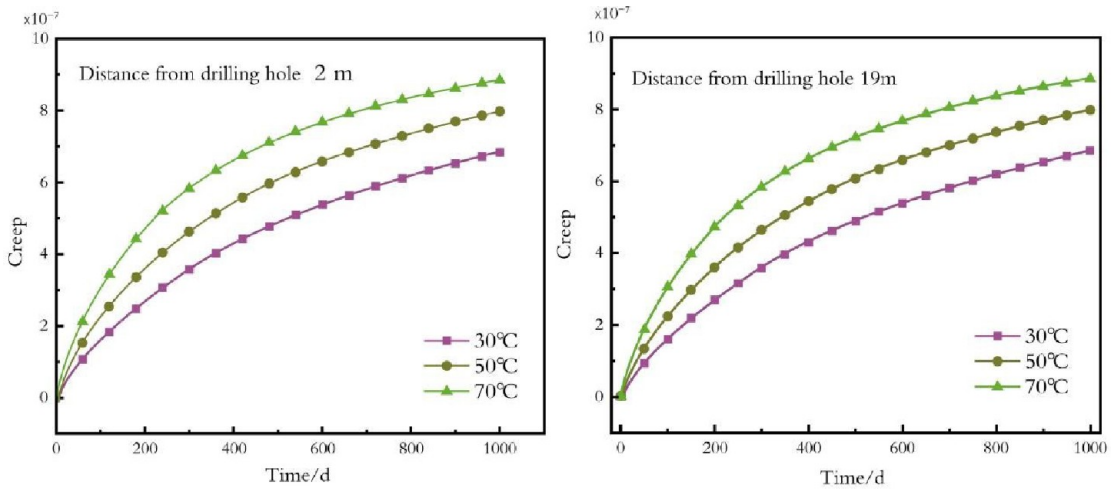

Figure 22. Creep deformation at different monitoring points at different temperatures

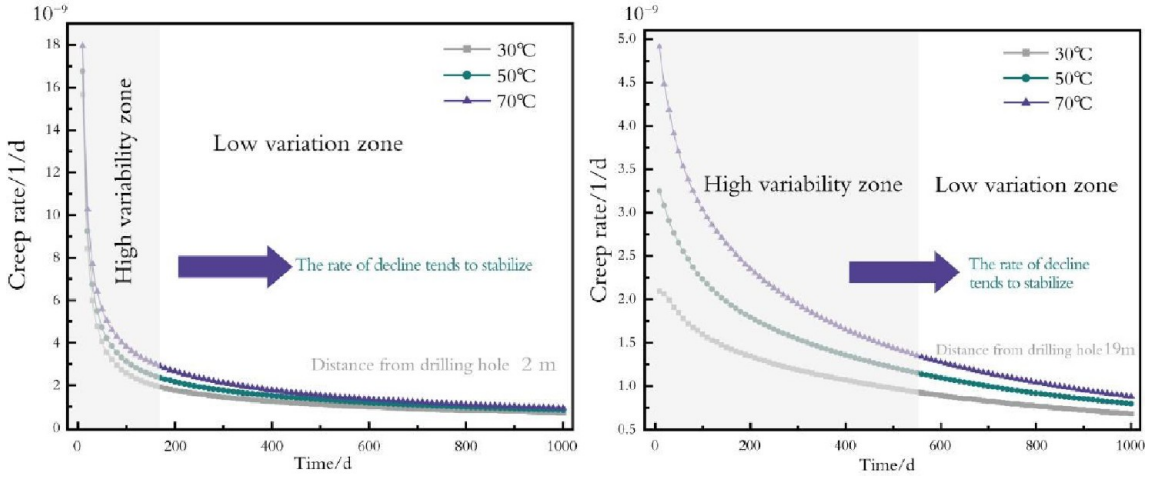

Figure 23. Creep rates at different monitoring points at different initial temperatures.

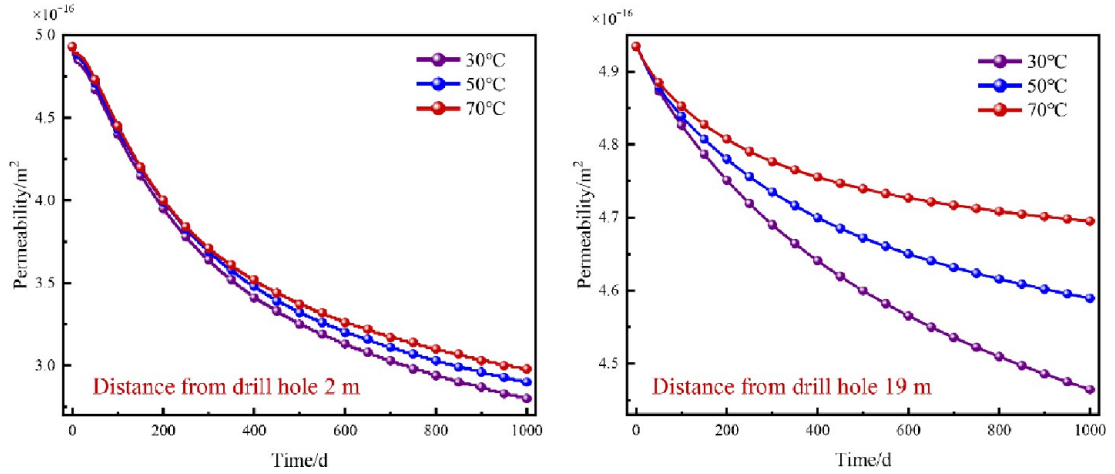

Figure 24. Permeability evolution of the coal seam at different monitoring points under different initial coal seam temperatures.

temperature; its creep deformation rate is also accelerated. The desorption far away from the borehole absorbs less heat, and the heat carried away by the free gas flow leads to a small and slow temperature change and slow creep deformation rate of coal here. During gas extraction at a later stage, the temperature field is almost in a state of equilibrium, which leads to the creep deformation evolution also tending to be stable, and the creep rate also shows an obvious trend of decline. In Figure 22, the creep rate varies greatly in the high-variability zone, while the creep rate changes slightly and tends to be stable in the low-variation zone. Considering the monitoring point with a distance of 2 m from the borehole,

https://doi.org/10.1021/acsomega.4c01706
ACS Omega 2024, 9, 22871−22891

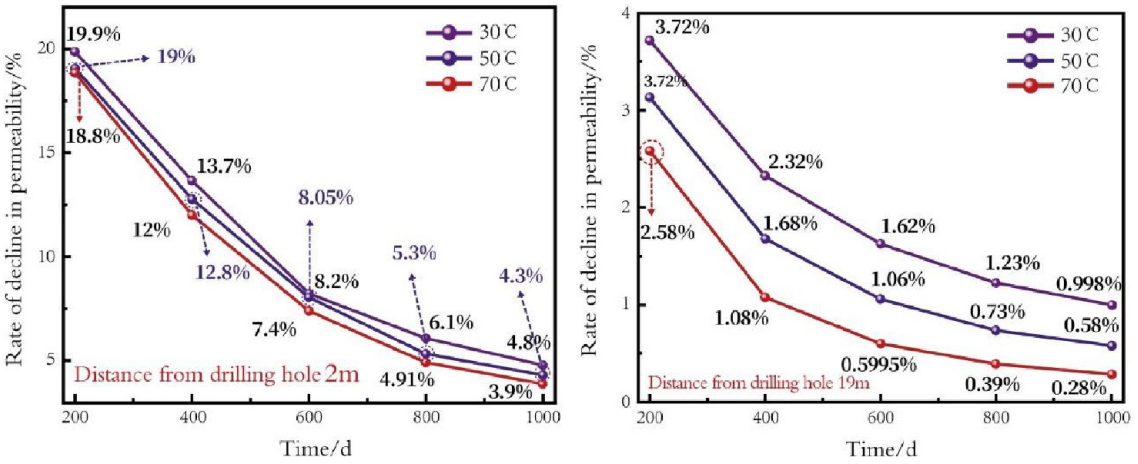

Figure 25. Permeability reduction ratio of the coal seam at different monitoring points under different initial coal seam temperatures.

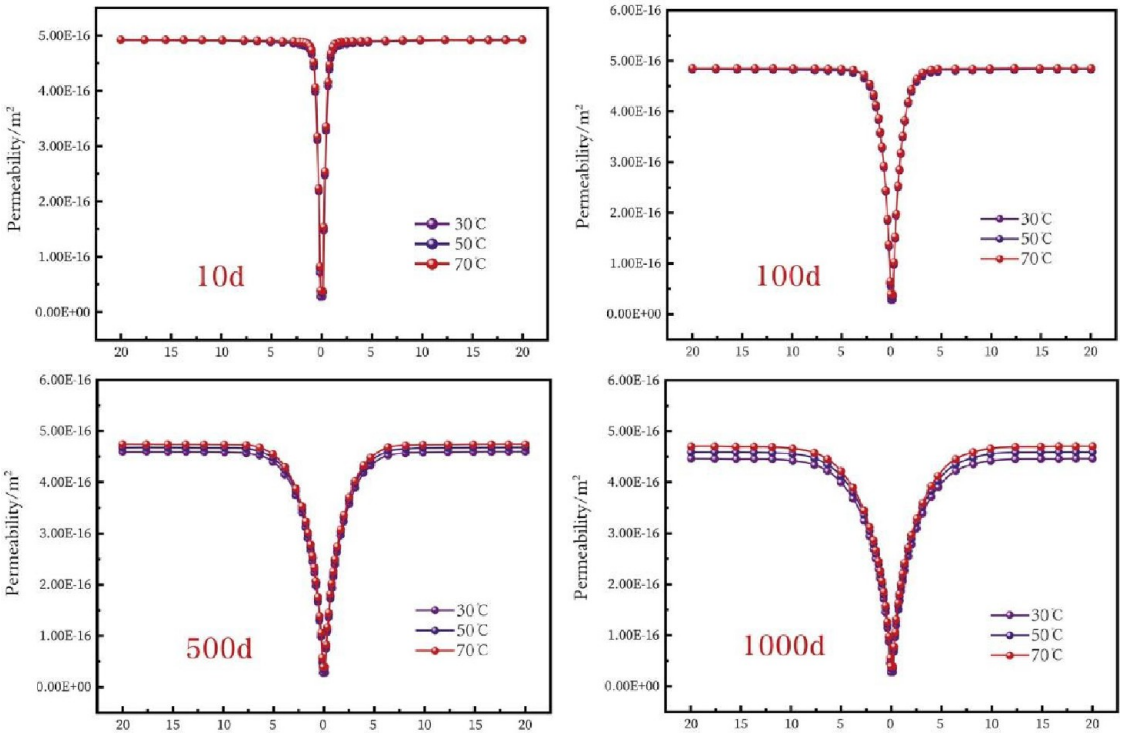

Figure 26. Permeability of the coal seam on the monitoring line under different initial coal seam temperatures.

there is an obvious difference between the high-variability zone and the low-variation zone, showing a trend of "high-variability zone is short and low-variation zone is long". At 19 m away, the high- and low-variation areas are almost the same length. This is because at a more proximate distance to the drilling hole at the initial extraction phase, the temperature will decrease significantly with the large amount of adsorbed gas desorption, which will enable a rising coal seam creep rate. In the middle and late stages of extraction, the temperature evolution becomes stable along with the equilibrium of gas desorption, so the creep rate becomes lower. The high-variability zone of the coal seam far away from the borehole becomes longer due to the gradual increase of gas desorption in the process of extraction, resulting in a low creep decline rate. The creep rate in the low-variation zone 19 m away from the borehole has not become flat, indicating that the farther away the coal body creep, the longer it takes to reach the stable state.

5.3. Effect of Temperature and Creep on Permeability. Temperature and creep's synergistic influences have a primary function in the evolution of permeability, and temperature also affects the degree of creep deformation. As the initial temperature of the coal seam increases, so does the coal seam's permeability, as Figure 24 depicts. As the time of extraction rises, the permeability decreases rapidly first and then slowly. This is because the coal seam's high initial temperature facilitates gas desorption, and an overabundance of gas desorption induces contraction and deformation of the coal matrix. Concurrently, as creep deformation increases, the coal seam opening decreases. The relationship between temperature and permeability is more pronounced in the case of coal seams characterized by elevated initial temperatures rather than creep deformation. In the early stage of

https://doi.org/10.1021/acsomega.4c01706
ACS Omega 2024, 9, 22871−22891

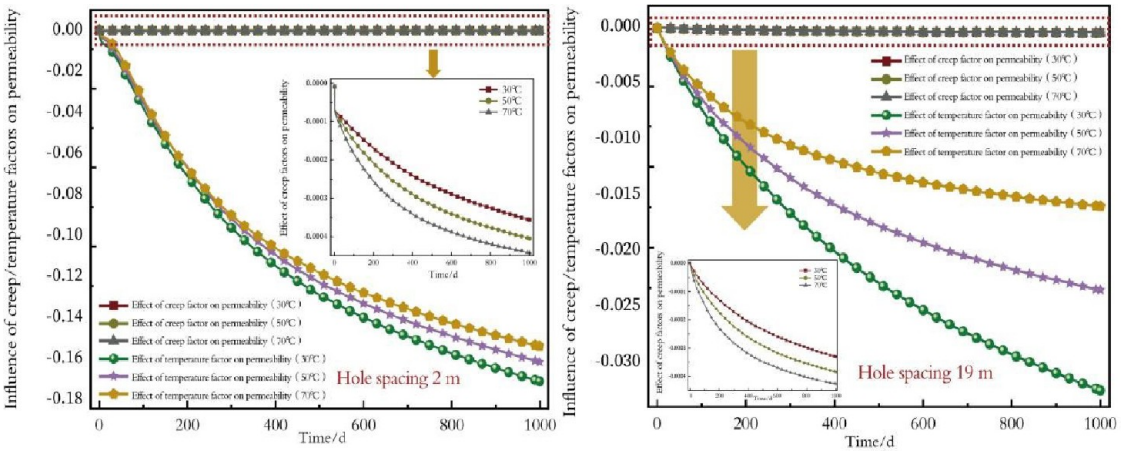

Figure 27. Effect of the creep and temperature on permeability.

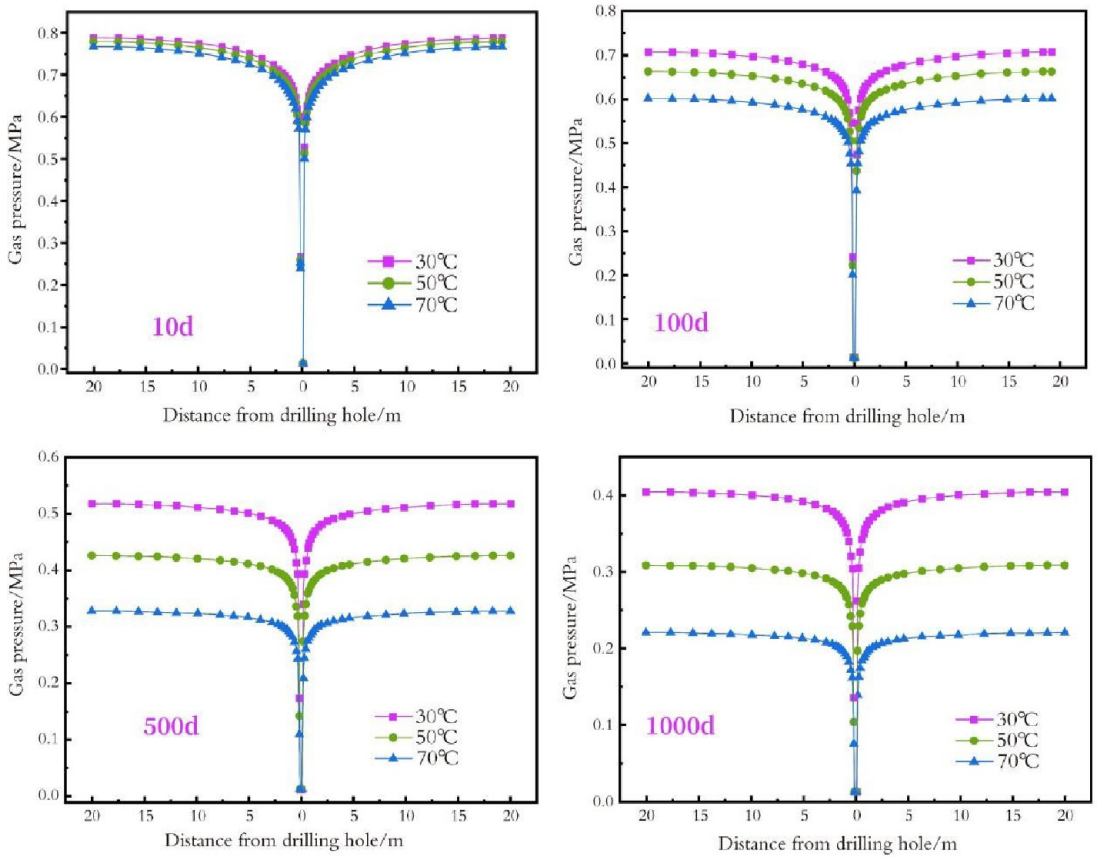

Figure 28. Variation of gas pressure at different extraction times on the same monitoring line.

extraction, the temperature of the coal seam decreases rapidly, while there is an accelerated rise in effective stress because of the gas pressure's rapid reduction, and the permeability decreases rapidly. In the middle and late stages of extraction, the temperature drop slowly leads to the creep deformation increase, and then the gas permeation channel narrows, and the permeability slowly decreases.

Figures 25 and 26 show the evolution of coal seam permeability near the hole. The greater pressure gradient of the coal seam in proximity to the borehole facilitates the desorption of gas and makes the matrix shrink, resulting in greater permeability changes. Stable gas pressure exists in the coal seam that is further from the borehole, and its desorption rate is low, which makes the permeability change less.

Figure 27 illustrates how temperature's impact on permeability is much greater than that of creep. This is because temperature can cause changes in gas adsorption and desorption, thermal expansion, gas flow, and creep. Permeability is influenced by temperature via a combination of many factors, including the influence of creep on permeability, indicating that the temperature and creep are dominant in the evolution of permeability.

5.4. Gas Pressure Field Distribution and Evolution. The diagram in Figure 28 illustrates the variation in the gas pressure throughout the process of extraction on the same

https://doi.org/10.1021/acsomega.4c01706
ACS Omega 2024, 9, 22871−22891

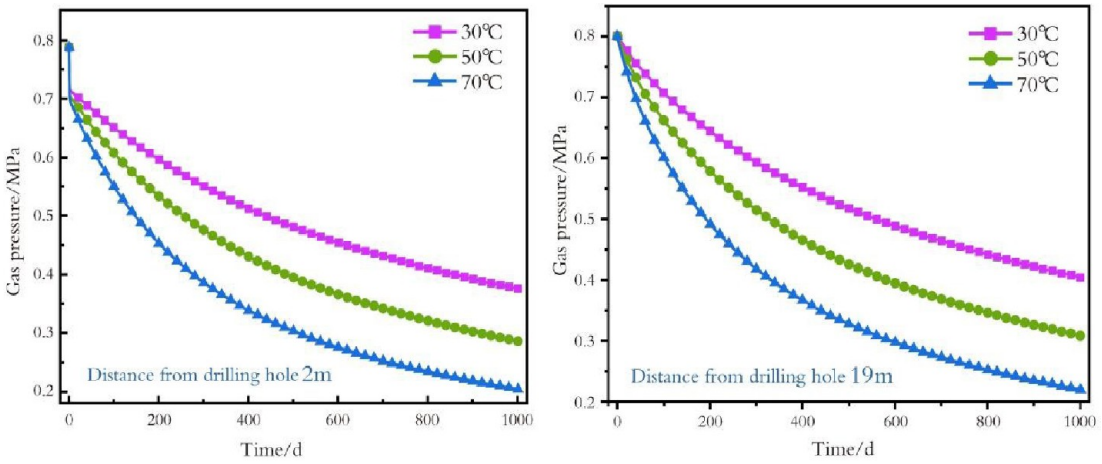

Figure 29. Pressure evolution curves with time at different monitoring points at different temperatures.

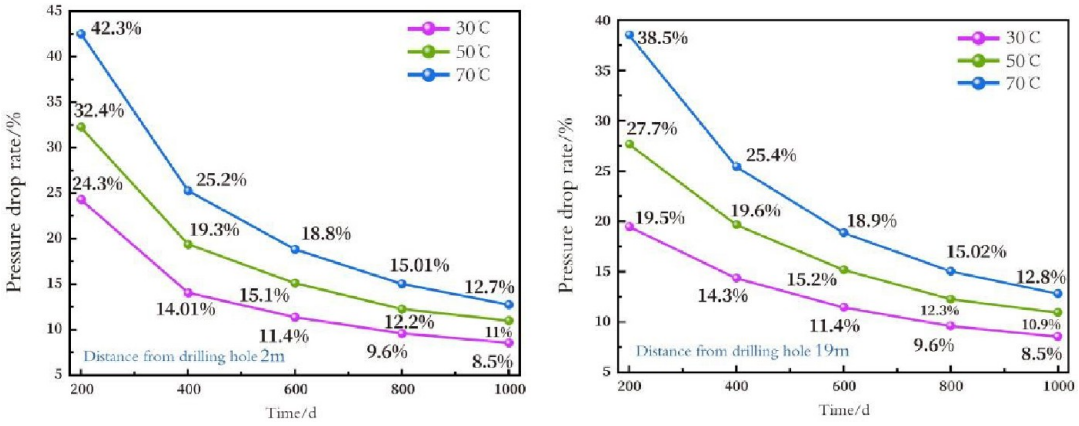

Figure 30. Pressure drop ratio at different monitoring points and different temperatures

monitoring line. It can be seen that the variation in gas pressure becomes more pronounced as one approaches the borehole, whereas it becomes less pronounced as one moves further away. This is because as one approaches the borehole, the pressure differential between the internal coal seam pressure and the pressure within the borehole increases, which promotes gas desorption. A large amount of free gas flows out through the borehole, and as a result, the change of gas pressure near the borehole is far greater than that far away from the borehole. Considering Figures 25, 26, and 27, the pressure change of the gas at the distance from the borehole and the initial temperature of the coal seam affect the gas pressure.

According to Figure 29, the gas pressure at the monitoring point 2 m from the borehole has a sudden change at the preliminary phase. The change trend in pressure at the point of monitoring with a distance of 2 m from the borehole is basically the same as that at 19 m away, with the pressure at the latter slightly higher than that at the former. From the above phenomenon, at gas extraction commencement, a large amount of adsorbed gas desorbs and leaves the coal seam, resulting in the pressure mutation. Due to the coal body's small and slow desorption when distant from the borehole, the small pressure and temperature change, the low permeability, and the slow gas transport, the pressure of the farther coal seam is slightly greater than the one more proximate.

Figure 30 shows the speed of the pressure drop at different extraction times under different initial coal seam temperatures. Accordingly, the pressure drop gradually slows down alongside extraction of gas. The maximum pressure drop ratio can reach 42.3%, and the minimum is 8.5%. This is because in the early stage of gas extraction, borehole's pressure discrepancy with the coal seam is large, and a large amount of adsorbed gas desorbs into free gas and flows out through the borehole. As the extraction of gas progresses, the borehole's pressure discrepancy with the coal seam decreases, the gas desorption rate decreases, and the coal seam pressure diminishes, which affects the effective stress and adsorption expansion deformation. The reduction in permeability influences the movement of gases. The ratio of pressure decrease to initial temperature of the coal seam increases. The initial coal bed temperature affects gas desorption. The higher the temperature is, as desorption increases, the initial gas extraction permeability likewise increases. The ratio of pressure decrease to initial coal fissure temperature increases proportionally. At a distance of 2 m from the borehole, at this monitoring point, when the initial coal seam temperature is 70 °C, the ratios of pressure drops every 200 days are 42.3%, 25.2%, 18.8%, 15.01%, and 12.7%, respectively. When away from the borehole by 19 m, at the same initial temperature of the coal seam, the ratios of pressure drops every 200 days are 38.5%, 25.4%, 18.9%, 15.02%, and 12.8%, respectively. It can be seen that the distance from the drilling hole has little influence on the gas drop ratio, and

https://doi.org/10.1021/acsomega.4c01706
ACS Omega 2024, 9, 22871−22891

pressure has greater sensitivity to change in temperature during the gas extraction process.

5.5. Gas Extraction Capacity. Gas extraction capacity and gas extraction rate are important indicators of the effect of gas extraction. Based on the multiphysical field coupling model constructed, this subsection is solved with the COMSOL software by setting different initial conditions. For the initial temperatures of the coal seam of 30, 50, and 70 °C, the gas extraction rate is computed by the multiphysical field coupling model.

Figure 31 shows the trend that with increasing extraction duration, the quantity of gas extracted also increases, and the growth rate gradually decreases. As for the coal seam temperature, the quantity of gas extracted exhibits an upward trend as the temperature rises (Figure 32). This is because in the early stage of gas extraction, as the temperature rises, gas desorption and contraction within the coal matrix intensify. Upon deformation caused by the combined effects of effective stress and adsorption, the crack opening at this time is larger, and its permeability is larger.

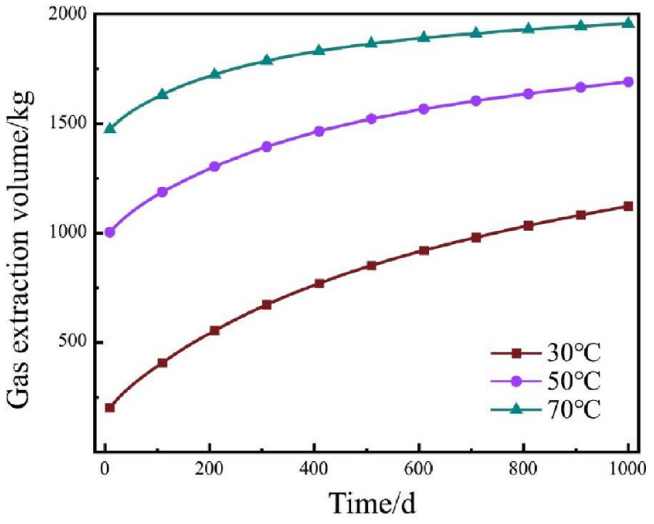

Figure 31. Gas extraction under different initial coal seam temperatures.

According to Figure 33, the gas extraction in the early fast mining area shows the characteristics of a high extraction rate. With the extension of gas extraction time, gas extraction gradually evolves to the slow extraction area, and its rate gradually stabilizes. This is because the temperature drop in the middle and late period of gas extraction leads to the creep deformation degree, and the gas desorption amount is smaller than in the early stage of gas extraction, and then the permeability evolves to a low level to reduce the gas transport capacity.

6. DISCUSSION

6.1. Verification of Coal Permeability Evolution Model under Thermal Effect. Based on the experimental data and theory, the coal permeability model, which considers creep, temperature, and matrix−crack interaction, can better describe the evolution law of coal permeability under multifield coupling. However, the validity and applicability of the MCT model are required to be further demonstrated. Through the creep and seepage test data considering the influence of temperature, the parameters in the coal permeability evolution model (eq 13) can be fitted to obtain the physical and mechanical parameters of coal, as shown in Table 3.

As can be seen from Figure 34, the coal permeability model (MCT model) established in this paper considering creep, temperature, and matrix−crack interaction has a good agreement with the experimental data, and the correlation coefficient can reach more than 90%. It is proved that the permeability model proposed in this paper can describe the

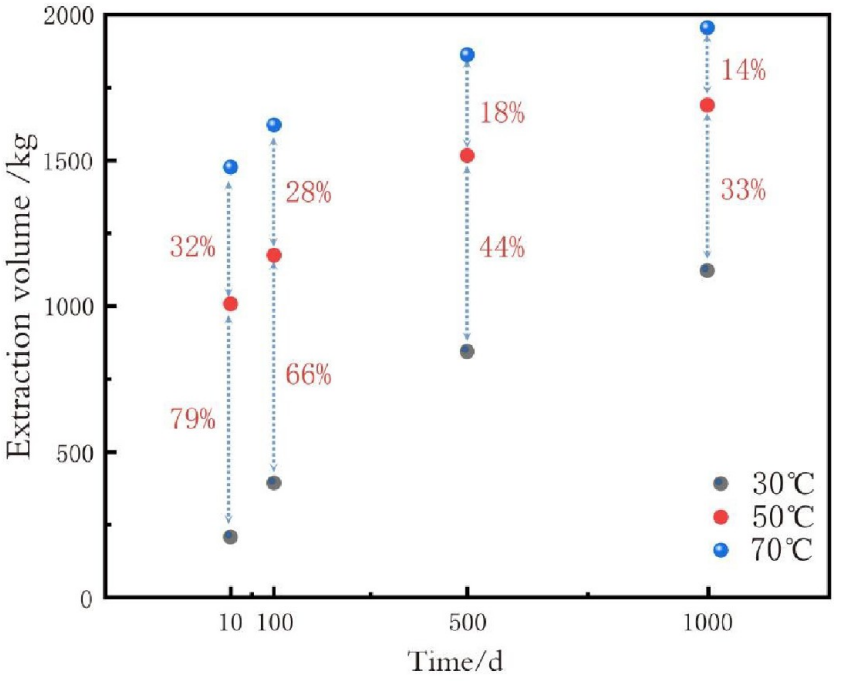

Figure 32. Rate of increase of extraction at different temperatures.

https://doi.org/10.1021/acsomega.4c01706
ACS Omega 2024, 9, 22871−22891

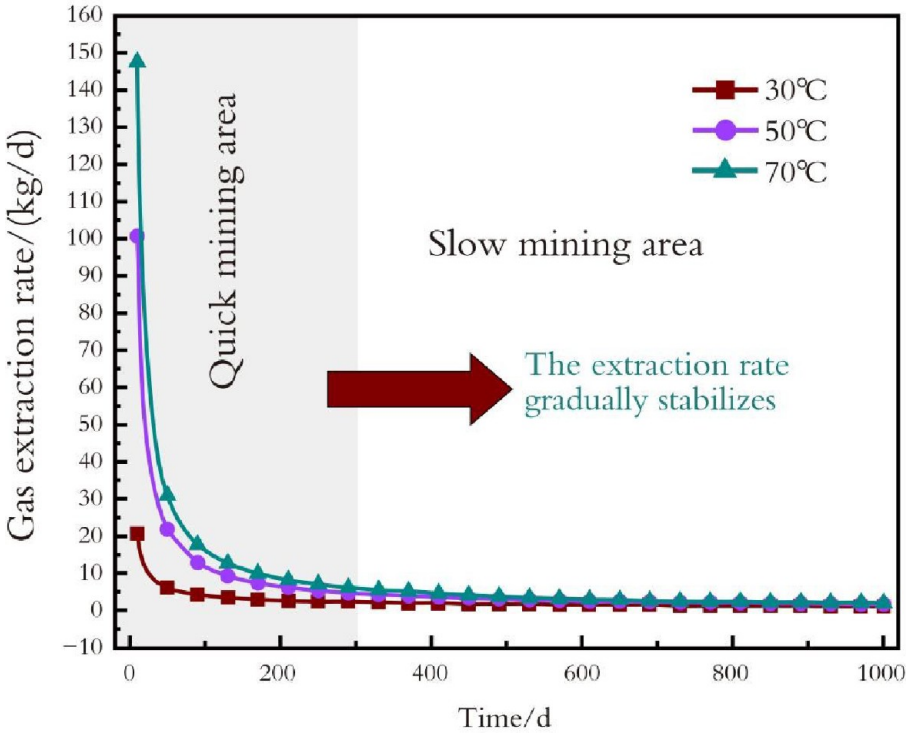

Figure 33. Gas extraction rate at different initial coal seam temperatures.

Table 3. Mechanical Parameters of Coal Samples

MCT model parameter	value		
	T = 30 °C	T = 50 °C	T = 70 °C
elasticity modulus (E_e) (GPa)	2.15	1.98	1.96
viscoelastic modulus (E_{ve}) (GPa)	1.79	1.72	1.70
coefficient of viscosity (η_{ve}) (GPa·h$^{\gamma}$)	3.21	3.08	2.97
Poisson's ratio (υ)	0.28	0.28	0.28
Biot coefficient (α)	1.00	1.00	1.00
adsorption pressure constant (P_L) (MPa)	10.0	10.0	10.0
temperature influence constant (a)	-1.1×10^{-3}	-1.6×10^{-3}	-1.3×10^{-3}
temperature influence constant (b)	0.26	0.24	0.20
coefficient of thermal expansion (α_1, α_T) (K^{-1})	1.0×10^{-4}	1.0×10^{-4}	1.0×10^{-4}
adsorption pressure coefficient (c_1) (MPa^{-1})	0.068	0.068	0.069
temperature coefficient (c_2) (K^{-1})	0.028	0.028	0.028
adsorption volume strain (ε_L)	0.002	0.002	0.002
initial voidage (ϕ_0)	0.91×10^{-3}	2.13×10^{-3}	3.74×10^{-3}
coupled internal expansion coefficient (f_{ST})	0.47	0.51	0.57
fractional derivative order (γ)	0.58	0.64	0.71

permeability evolution law of the creep and seepage process under different temperature conditions.

6.2. Permeability Evolution Analysis at Different Temperatures Based on MCT Model. According to eq 13 and the MCT model parameter data in Table 3, permeability

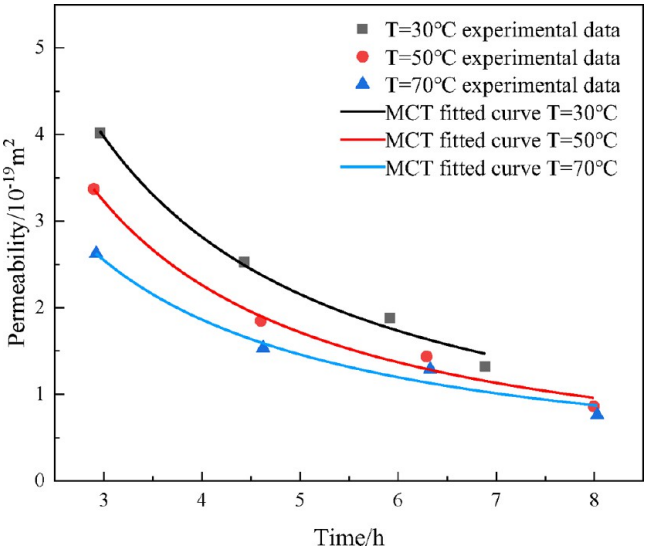

Figure 34. Permeability evolution of the MCT model and experimental results under creep condition.

evolution curves under different temperature conditions are drawn, as shown in Figure 35. As can be seen from Figure 35, considering only the influence of temperature on the permeability of coal, the initial permeability of coal gradually decreases with the increase of temperature. When the temperature is 50 °C, the initial permeability of coal is 28.36 $\times$ 10^{-19} m^2. When the temperature is 60 °C, the initial permeability of coal is 12.35 $\times$ 10^{-19} m^2. When the temperature is 70 °C, the initial permeability of coal is 3.88 $\times$ 10^{-19} m^2. It can be seen that the increase of temperature leads to the enhancement of gas desorption ability, which in turn leads to the decrease of adsorption expansion deformation

https://doi.org/10.1021/acsomega.4c01706
ACS Omega 2024, 9, 22871−22891

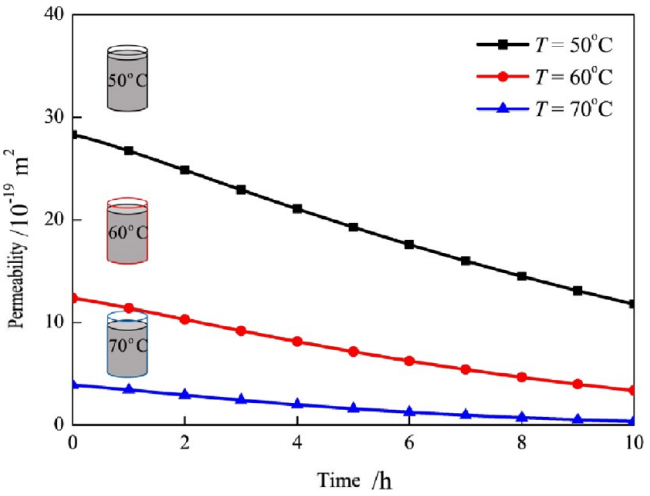

Figure 35. Permeability evolution at different temperatures.

ability of the coal matrix, which leads to the attenuation of coal permeability.

7. CONCLUSIONS

This paper studies the influence of coal deformation on permeability under high temperature and analyzes the influence of creep deformation on permeability evolution and the influence of creep deformation under under different temperature conditions. A permeability model (MCT permeability model) based on creep deformation, temperature influence, and matrix−cleft interaction is established. By establishing the multiphysical field permeability evolution model considering diffusion field, seepage field, stress field, and temperature field, the paper analyzes the mechanism of temperature deformation, the relationship between creep deformation and temperature and pressure, creep deformation's effect on permeability, dynamic gas pressure distribution, and gas extraction variation. The following conclusions can be drawn:

(1) In order to quantify temperature's effect on coal permeability and internal pore structure, with respect to thermodynamics and rock mechanics theory, the coal porosity model is established from the perspectives of thermal expansion deformation, creep deformation, and gas adsorption.

(2) A direct association arises in axial creep deformation with respect to temperature. Due to the influence of temperature, thermal damage occurs in the coal body, which deteriorates coal's physical properties, thus leading to higher deformation due to axial creep. Because of rising test temperature, the gas desorption ability is enhanced, and the expansion and deformation of the coal matrix lead to intracompression of the coal body, which suppresses its penetration ability.

(3) By setting the initial temperature of different coal seams by COMSOL Multiphysics software, the data of the evolution of temperature field, creep deformation, permeability change, gas pressure, and extraction amount can be obtained. By analyzing these data, as the initial temperature of the coal seam increases, the rate of temperature change accelerates, creep deformation becomes more pronounced, permeability decline decelerates, gas pressure decreases more rapidly, and gas volume extraction increases. The maximum temperature of the initial coal seam set in this paper is 70 °C; 0.8 MPa is the preliminary gas pressure within the coal seam; the gas pressure can drop to 0.022 MPa after 1000 days of gas extraction; and the gas extraction capacity is 1956 kg. These data are larger than the initial coal seam temperature of 30 and 50 °C. At the same time, it is found that temperature's effect on permeability is much greater than that of creep deformation, and the high initial coal temperature is conducive to gas extraction.

AUTHOR INFORMATION

Corresponding Author

Naifu Cao − *China Coal Research Institute, Beijing 100013, China; Chinese Institute of Coal Science, Beijing 100013, China; Mine Intelligent Ventilation Division, CCTEG China Coal Research Institute, Beijing 100013, China;* orcid.org/0000-0002-9345-6052; Email: 1424046831@qq.com

Authors

Pengfei Jing − *China University of Mining & Technology (Beijing), Beijing 100083, China*

Zhonggang Huo − *China Coal Research Institute, Beijing 100013, China; Mine Intelligent Ventilation Division, CCTEG China Coal Research Institute, Beijing 100013, China*

Yuntao Liang − *China Coal Research Institute, Beijing 100013, China; Chinese Institute of Coal Science, Beijing 100013, China*

Lang Zhang − *China Coal Research Institute, Beijing 100013, China; Mine Intelligent Ventilation Division, CCTEG China Coal Research Institute, Beijing 100013, China*

Complete contact information is available at: https://pubs.acs.org/10.1021/acsomega.4c01706

Notes

The authors declare no competing financial interest.

ACKNOWLEDGMENTS

The authors gratefully acknowledge the financial support from the National Natural Science Foundation of China (5217042662) and on-site technical guidance and treatment of problems from technical staff in Coal and Transportation Industry Management Department, China Energy Investment Group.

REFERENCES

(1) Tian, F.; Liu, Z.; Zhu, W.; Su, W.; Wang, J.; Yang, J.; Zhang, Z. Experimental Assessment of Combined Contribution of Coal Mass Diffusion and Seepage to Methane Migration under In Situ Stress Conditions. *Energy Fuels* **2023**, *37* (8), 5766−5776.

(2) Zhang, L. Q. Study on the law of coal rupture and gas seepage in coal seam gas extraction. Ph.D. Thesis, China University of Mining and Technology, 2020.

(3) Liu, H. H. Evolution characteristic of the main control factor of coal body gas seepage and its control mechanism for gas extraction. Ph.D. Thesis, China University of Mining and Technology, 2020.

(4) Yuan, D. S. Gas desorption and seepage of low rank coal seam and its control mechanism for gas extraction. Ph.D. Thesis, China University of Mining and Technology, 2018.

(5) Seidle, J. P.; Jeansonne, M. W.; Erickson, D. J. Application of matchstick geometry to stress dependent permeability in coals.

Presented at the SPE Rocky Mountain Regional Meeting, Casper, Wyoming, 1992; Paper SPE-24361-MS. DOI: 10.2118/24361-MS
(6) Seidle, J. R.; Huitt, L. G. Experimental measurement of coal matrix shrinkage due to gas desorption and implications for cleat permeability increases. Presented at the International Meeting on Petroleum Engineering, Beijing, China, 1995; Paper SPE-30010-MS. DOI: 10.2118/30010-MS
(7) Liu, Z.; Cheng, Y.; Wang, L.; Wang, H.; Jiang, J.; Li, W. Analysis of coal permeability rebound and recovery during methane extraction: Implications for carbon dioxide storage capability assessment. *Fuel* **2018**, *230*, 298−307.
(8) Harpalani, S.; Chen, G. Effect of gas production on porosity and permeability of coal. In *Symposium on Coalbed Methane Research and Development in Australia*; James Cook University of North Queensland, 1992; pp 67−73
(9) Palmer, I.; Mansoori, J. How permeability depends on stress and pore pressure in coalbeds: a new model. *SPE Reservoir Eval. Eng.* **1998**, *1* (06), 539−544.
(10) Ghazvinian, A.; Sarfarazi, V.; Schubert, W.; Blumel, M. A study of the failure mechanism of planar nonpersistent open joints using PFC2D. *Rock Mech. Rock Eng.* **2012**, *45*, 677−693.
(11) Heuze, F. E. High-temperature mechanical, physical and thermal properties of granitic rocks-a review. *Int. J. Rock Mech. Min. Sci.* **1983**, *20*, 3−10.
(12) Glover, P. W. J.; Baud, P.; Darot, M.; Meredith, P. G.; Boon, S. A.; LeRavalec, M.; Zoussi, S.; Reuschle, T. α/β phase transition in quartz monitored using acoustic emissions. *Geophys. J. Int.* **1995**, *120* (3), 775−782.
(13) Chopra, P. N. High-temperature transient creep in olivine rocks. *Tectonophysics* **1997**, *279*, 93−111.
(14) Zhang, Z.X.; Yu, J.; Kou, S.Q.; Lindqvist, P.-A. Effects of high temperature on dynamic rock fracture. *Int. J. Rock Mech. Min. Sci.* **2001**, *38*, 211−225.
(15) Cai, T. T., Experimental study on coal rheological-seepage characteristics under the action of heat-force coupling. Ph.D. Thesis, Taiyuan University of Technology, 2018.
(16) Li, L. C.; Yang, T. H.; Tang, C. A.; Wang, D. G. TMD coupling numerical model of rock rupture process. *Rock Soil Mech.* **2006**, *27* (10), 727−732.
(17) Luo, J. A.; Wang, L. G.; Tang, F. R.; He, Y.; Zheng, L. Variation in the temperature field of rocks overlying a high-temperature cavity during underground coal gasification. *Min. Sci. Technol. (China)* **2011**, *21*, 709−713.
(18) Zhang, Y.; Niu, K.; Du, W.; Zhang, J.; Wang, H.; Zhang, J. A method to identify coal spontaneous combustion-prone regions based on goaf flow field under dynamic porosity. *Fuel* **2021**, *288*, 119690.
(19) Liu, Z.; Lin, X.; Cheng, Y.; Chen, R.; Zhao, L.; Wang, L.; Li, W.; Wang, Z. Experimental investigation on the diffusion property of different form coal: Implication for the selection of CO_2 storage reservoir. *Fuel* **2022**, *318*, 123691.
(20) Yang, D.; Sarhosis, V.; Sheng, Y. Thermal−mechanical modelling around the cavities of underground coal gasification. *J. Energy Inst.* **2014**, *87* (4), 321−329.
(21) Lu, Y. L.; Wang, L. G.; Tang, F. R.; He, Y.; Zheng, L. Evolution of rock fissure in combustion zone under temperature-stress coupling during underground coal gasification. *Coal J.* **2012**, *37* (8), 1292−1298.
(22) Kong, X. Y.; Li, D. L.; Xu, X. Z.; Lu, D. T. A mathematical model of heat-flow-solid coupling seepage. *Hydrodyn. Res. Prog.* **2005**, *20* (2), 269−275.
(23) Wei, C. H. Coal body damage model and its application. Ph.D. Thesis, Northeastern University, 2012.
(24) Wang, L. J. Modeling Approach to Creep-Seepage-Temperature Coupling in Deep Coal. Ph.D. Thesis, China University of Mining and Technology, 2019.
(25) Cheng, Y.; Liu, Q.; Ren, T. *Coal Mechanics*; Springer, 2021.
(26) Zhang, L.; Zhou, H.; Wang, X.; Zhao, J.; Ju, Y.; Deng, T. On Permeability Evolution of Coal Induced by Temperature, Creep, and Matrix−Fracture Interaction. *Energy Fuels* **2022**, *36* (3), 1470−1481.
(27) Wang, J.; Lian, W.; Li, P.; Zhang, Z.; Yang, J.; Hao, X.; Huang, W.; Guan, G. Simulation of pyrolysis in low rank coal particle by using DAEM kinetics model: reaction behavior and heat transfer. *Fuel* **2017**, *207*, 126−135.
(28) Mora, C. A.; Wattenbarger, R. A. Analyst and verification of dual porosity and CBM shape factors. Presented at the Canadian International Petroleum Conference, Calgary, Alberta, June 2006; Paper PETSOC-2006-139. DOI: 10.2118/2006-139.
(29) Wang, L. G. Gas injection drives the deep coal seam CH_4 Experiments and characteristic-after after study. Ph.D. Thesis, China University of Mining and Technology, 2013.
(30) Zhu, W. C.; Wei, C. H.; Liu, J.; Qu, H. Y.; Elsworth, D. A model of coal-gas interaction under variable temperatures. *Int. J. Coal Geol.* **2011**, *86* (2−3), 213−21.
(31) Wu, Y.; Liu, J.; Chen, Z.; Elsworth, D.; Pone, D. A dual poroelastic model for CO_2-enhanced coalbed methane recovery. *Int. J. Coal Geol.* **2011**, *86* (2−3), 177−89.
(32) Fan, Y.; Deng, C.; Zhang, X.; Li, F. Q.; Wang, X. Y.; Qiao, L. Numerical study of CO_2-enhanced coalbed methane recovery. *Int. J. Greenhouse Gas Control* **2018**, *76*, 12−23.
(33) Li, S.; Fan, C.; Han, J.; et al. A fully coupled thermal-hydraulic-mechanical model with two-phase flow for coalbed methane extraction. *J. Nat. Gas Sci. Eng.* **2016**, *33*, 324−36.
(34) Wang, K.; Wang, L.; Ju, Y.; Dong, H. Z.; Zhao, W.; Du, C. G.; Guo, Y. Y.; Lou, Z.; Gao, H. Numerical study on the mechanism of air leakage in drainage boreholes: A fully coupled gas-air flow model considering elastic-plastic deformation of coal and its validation. *Process Saf. Environ. Prot.* **2022**, *158*, 134−145.
(35) Zhang, L. P. Research on thermal-fluid-solid coupling mechanism and application of low permeability coalbed methane mining. Ph.D. Thesis, China University of Mining and Technology, 2011.
(36) Cui, X.; Bustin, R. M. Volumetric strain associated with methane desorption and its impact on coalbed gas production from deep coal seams. *AAPG Bull.* **2005**, *89*, 1181−1202.
(37) Zhou, H.; Zhang, L.; Wang, X.; Rong, T.; Wang, L. Effects of matrix−fracture interaction and creep deformation on permeability evolution of deep coal. *Int. J. Rock Mech. Min. Sci.* **2020**, *127*, 104236.
(38) Zhang, L.; Zhou, H.; Wang, X.; Wang, L.; Su, T.; Wei, Q.; Deng, T. A triaxial creep model for deep coal considering temperature effect based on fractional derivative. *Acta Geotech.* **2022**, *17*, 1739−1751.

https://doi.org/10.1021/acsomega.4c01706
ACS Omega 2024, 9, 22871−22891